

DTIC FILE COPY

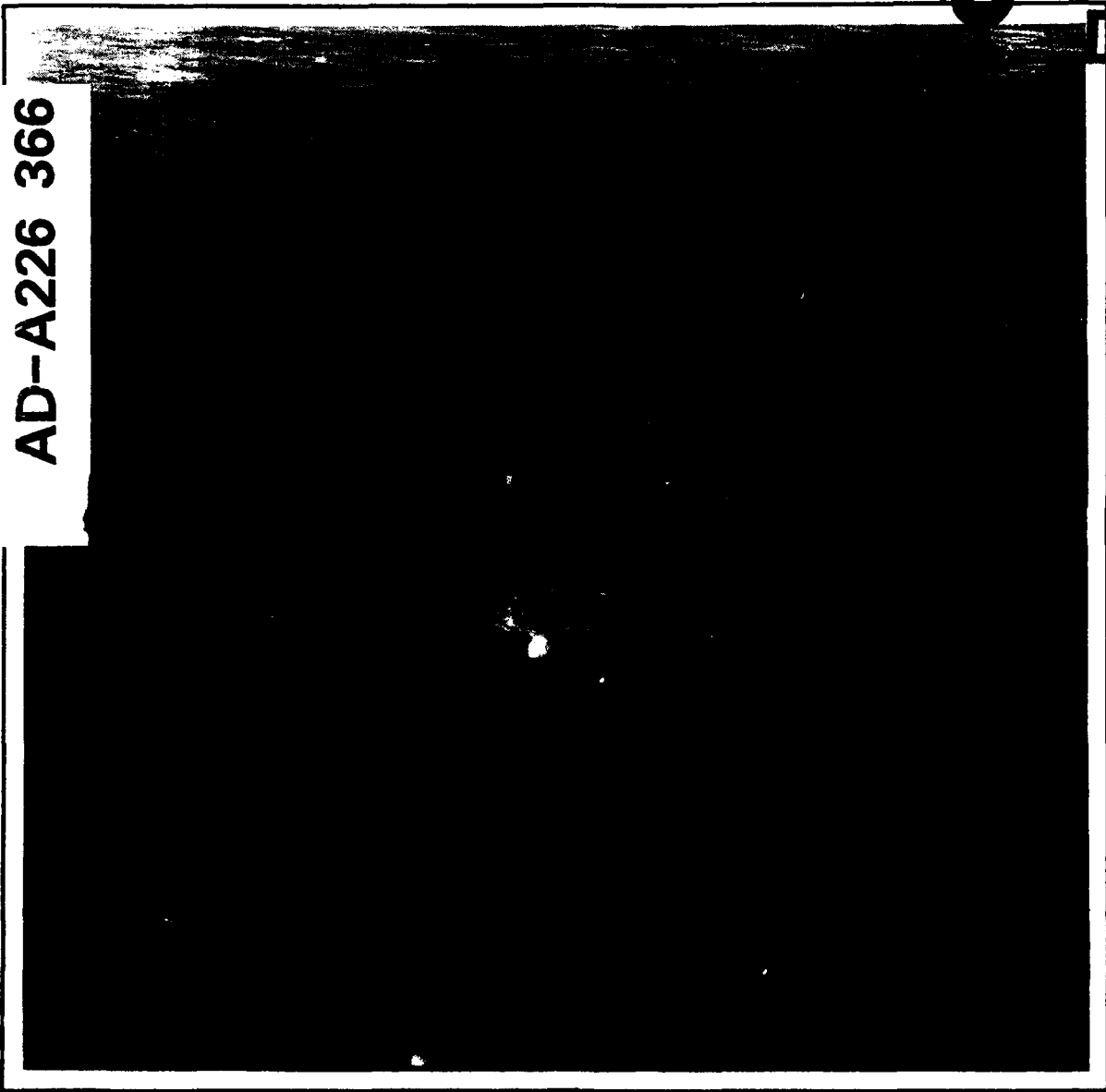
(1)

SAXON I

(SAR AND X-BAND OCEAN NONLINEARITIES)
SCIENCE PLAN

S DTIC
ELECTE
SEP 06 1990 **D**

AD-A226 366



Approved for Public Release; Distribution Unlimited

90 09 05 056

SECURITY CLASSIFICATION OF THIS PAGE (When Data Entered)

REPORT DOCUMENTATION PAGE		READ INSTRUCTIONS BEFORE COMPLETING FORM
1. REPORT NUMBER	2. GOVT ACCESSION NO.	3. RECIPIENT'S CATALOG NUMBER
4. TITLE (and Subtitle) SAXON I Science Plan 1988/1990		5. TYPE OF REPORT & PERIOD COVERED SAXON Science Plan 1988/1990
7. AUTHOR(s) Omar H. Shemdin and Les McCormick with SAXON Experiment Team		6. PERFORMING ORG. REPORT NUMBER
9. PERFORMING ORGANIZATION NAME AND ADDRESS Ocean Research and Engineering 255 South Marengo Ave. Pasadena, California 91101		8. CONTRACT OR GRANT NUMBER(s) NOO14-86-C-0303
11. CONTROLLING OFFICE NAME AND ADDRESS Office of Naval Research 800 N. Quincy Street Arlington, VA 22217		10. PROGRAM ELEMENT, PROJECT, TASK AREA & WORK UNIT NUMBERS 0810-Physical Oceanography 0803-Dynamic Oceanography 1709-Radar Detection
14. MONITORING AGENCY NAME & ADDRESS (if different from Controlling Office)		12. REPORT DATE August 1988
		13. NUMBER OF PAGES
		15. SECURITY CLASS. (of this report) Unclassified
		15a. DECLASSIFICATION/DOWNGRADING SCHEDULE
16. DISTRIBUTION STATEMENT (of this Report) Approved for public release, distribution unlimited.		
17. DISTRIBUTION STATEMENT (of the abstract entered in Block 20, if different from Report)		
18. SUPPLEMENTARY NOTES		
19. KEY WORDS (Continue on reverse side if necessary and identify by block number) Synthetic Aperture Radar, Radar Backscatter, Surface Waves, Capillary Waves, Internal Waves, Ship Wakes.		
20. ABSTRACT (Continue on reverse side if necessary and identify by block number) This is a follow-on to the TOWARD experiment which was executed in 1984-1986 to provide experimental verification of the mechanisms responsible for SAR imaging of the ocean surface. The TOWARD experiment provided a data set that is adequate for resolving the most important issues related to SAR imaging of surface waves at L-Band.		

Unclassified

SECURITY CLASSIFICATION OF THIS PAGE (When Data Entered)

The mechanisms involved in SAR imaging at X-Band are far less understood (C-Band is in near proximity of X-Band). The SAXON experiment, although similar in scope to TOWARD, addresses the nonlinear hydrodynamics associated with the very short surface waves (0.5 - 5 cm in length), and radar backscatter from the ocean surface at X-Band and higher frequencies.

K...

[...]

S-N 0102-LF-014-6601

Unclassified

SECURITY CLASSIFICATION OF THIS PAGE(When Data Entered)

SAXON I

(SAR X-BAND AND OCEAN NONLINEARITIES)

(1988/1990)

SCIENCE PLAN



Accession For	
NTIS CRA&I	<input checked="" type="checkbox"/>
DTIC TAB	<input type="checkbox"/>
Unannounced	<input type="checkbox"/>
Justification	
By _____	
Distribution /	
Availability Codes	
Dist	Avail and/or Special
A-1	

Prepared by:

O. H. SHEMDIN
Principal Investigator

L. D. Mc CORMICK
Test Director

Ocean Research and Engineering
255 South Marengo Avenue
Pasadena, California 91101

August 1988

(Cover: Circular Wave Generator, also Known
as "Bobbing Buoy", is Operated in SAXON)

ACKNOWLEDGEMENT

This Science Plan is based on a "Straw Man" plan presented by Dr. O. H. Shemdin at a meeting of investigators held in La Jolla, California on 16-17 July 1987. Contributions were provided by the attendees through discussion and submission of work statements and viewgraphs. A second planning meeting was held 25-26 February 1988 in Pasadena, California for review of the loss of the OCNR Tower in a major storm. Careful consideration was given to the Chesapeake Light Tower, located outside of the Chesapeake Bay entrance on the East Coast, as the alternate site for the SAXON I experiment. The experiment is sponsored by the Office of Naval Research under the joint sponsorship of the SAR Program with Commander T.S. Nelson as Program Manager and Mr. H. Dolezalek as Technical Monitor of the ocean SAR effort, and the Marine Microlayer Accelerated Research Initiative (ARI) Program with Dr. F. Herr as Program Manager.

EXECUTIVE SUMMARY

Synthetic Aperture Radar (SAR) provides high resolution imaging of the ocean surface independent of sunlight and under most weather conditions. SAR images can be processed to yield useful information on directional properties of surface waves, internal waves, location of boundary currents, wind speed and ship wakes. The spaceborne wide-swath high-resolution imaging capability in global orbit allows detection of these processes in both meso- and global scales.

To transform the SAR into a useful tool, and to understand the limits of its validity, it is necessary to understand the process by which an ocean surface is transformed to the image or another form of output signal. To this end all significant elements of the transformation process, including extraneous influences, must be either quantitatively known or be measured. For Synthetic Aperture Radar, as an instrument to image or provide a measure of the ocean surface (and after the TOWARD, SARSEX and LEWEX Experiments), the still unknown elements are mostly in the area of surface and subsurface hydrodynamics, and in certain aspects of radar backscatter from the ocean surface. The main objective of future experiments, of which SAXON I is one, is to measure these elements.

The TOWARD experiment was executed in 1984-1986 to provide experimental verification of mechanisms responsible for SAR imaging of the ocean surface. This experiment provided a data set that is adequate for resolving the most important issues related to SAR imaging of surface waves at L-Band. The data set also provided insights on issues related to SAR imaging of internal waves, imaging of the ocean surface with X-Band radars and the influence of the microlayer.

The mechanisms involved in SAR imaging at X-Band are far less understood (C-Band is in near proximity of X-Band). Here, an experiment similar in scope to TOWARD is presented to understand the hydrodynamics and radar backscatter processes associated with the very short surface waves (0.5 - 5 cm in length). For this purpose a stable platform is mandatory for generating credible hydrodynamic (directional wave height and slope spectra) and radar backscatter data (obtained at fixed incidence angles). The insights gained in TOWARD at L-Band, in determining the transfer function from a radar backscatter map to a SAR scene, are potentially applicable to X-Band. That is, the SAR imaging model derived for L-Band can be extended in frequency to X-Band. However, the primary issues at X-Band relate to the hydrodynamics of the very short waves which are strongly nonlinear. This is clearly indicated in the Probability Density Functions (PDF) obtained with the laser slope

sensor. The radar backscatter measurements at X-Band and higher frequencies also show different characteristics, such as frequency of spikes, compared to those at L-Band.

A basic X-Band experiment, similar in scope to TOWARD, is planned here as a follow-on to TOWARD. The experiment is given the acronym SAXON I to stress SAR X-Band and Ocean Nonlinear aspects of SAR imaging of the ocean surface. The Chesapeake Tower located on the East Coast, offshore of the Chesapeake Bay entrance is selected as the stable platform for deployment of near surface sensors. This site is selected following an intensive review of available towers, to replace the NOSC Tower, subsequently named the OCNR Tower, after its destruction in a major storm on 18 January 1988. The Chesapeake Tower site is a most representative alternative to the abandoned site. The plan calls for the following suite of measurements:

1. Directional properties of short surface waves by in-situ capillary wave sensors, stereophotography and Stillwell-type photography. A scanning-beam laser-optical sensor is used as the in-situ sensor.
2. Radar backscatter measurements from the ocean surface in the range 5-95 GHz. Single and multi-frequency radars are used in parallel to provide frequency coverage.
3. RAR and SAR images are obtained simultaneously over the instrumented areas. It is planned that coverage be provided by 1) NRL RP-3A, and 2) NADC RP-3A to include L- C-, and X-Band SAR and X-Band RAR.

The SAXON I experiment is to address the following tasks (consistent with many key recommendations in the SAR Working Group Report, 1986):

1. Determine the modulation of centimeter waves by long surface waves and by internal waves. Included in this determination is the influence of the intermediate surface waves (0.5-10m in length).
2. Validate existing hydrodynamic models (e.g. Hughes, 1978) on modulation of centimeter waves by long surface waves and by internal waves.
3. Determine the modulation of radar backscatter from the ocean surface induced by surface and/or internal waves propagating through the radar footprint. The emphasis is on radar frequencies in the range 10-95 GHz.

4. Test radar backscatter models by using short surface waves as input, and comparing the output with measurements.
5. Test validity of the TOWARD SAR imaging theory (validated at L-Band) for X-Band and higher frequencies.
6. Specific experiments are appended to compare accuracy and resolution of optical and passive microwave techniques in detecting modulations on the ocean surface induced by natural or man-made processes.
7. Applied experiments are appended, such as ocean surface effects in the wake of ships, provided that they amplify the basic objectives stated above.

The present plan indicates participation by twenty-six (26) independent research organizations. These are detailed in Section IV under Participation. The SAXON I experiment is executed from the Chesapeake Light Tower (CLT) in September 1988, with data analysis and evaluation of results to extend into 1990.

TABLE OF CONTENTS

	PAGE
EXECUTIVE SUMMARY	iii
I. INTRODUCTION	1
II. SCIENTIFIC OBJECTIVES	6
III. THE FIELD SITE	12
IV. PARTICIPATION	21
V. FIELD MEASUREMENTS	24
VI. FIELD SITE INSTRUMENT MOUNTINGS	43
VII. EXPERIMENT COORDINATION AND MEASUREMENT STRATEGY	44
VIII. DATA MANAGEMENT	49
IX. DATA ANALYSIS	51
REFERENCES	54
APPENDIX A (DATA ON OTHER AIRCRAFT)	56
APPENDIX B (SAXON I DIRECTORY)	71

LIST OF FIGURES

FIGURE	PAGE
1. Location of Chesapeake Light Tower, Depth Contours in Meters. The Solid Lines Specify Nominal Flight Track Over the Tower	14
2. Recent Photograph of Chesapeake Light Tower as Seen from the South	15
3. Side View of Chesapeake Light Tower as Seen from the North Showing Elevation Levels. The Bottom is Now at -15m	16
4. Catwalk Surrounding Chesapeake Tower at 5m Level Above MLW	17
5. View of U.S. Coast Guard Helicopter Landing on the Helicopter Deck	18
6.. Surface Climatology in the Chesapeake Tower Vicinity as Provided by U.S.Coast Guard Wind and Wave Summary Report No. CC-D-05-84 for the Months of July-September	20
7. Surface Climatology in the Chesapeake Tower Vicinity as Provided by U.S.Coast Guard Wind and Wave Summary Report No. CC-D-05-84 for the Months of October-December	21
8. Wave Follower System in Operation with the Wave-Slope Sensor	26
9. Sketch of Laser Beam Acceptance Cones	27
10. Schematic of Stereo-Geometry. The Cameras Show the T-Bar in Their Field of View for Calibration	29
11. Capacitance Wave Probe Spar Buoy	33
12. Flight Patterns for SAR and RAR	37
13. Schematic of a Typical Ship Pass	42
14. View of Instruments Mounted, as Seen Looking Downward at Base of Tower, -6m Level. 1. Wave Slope Sensor-(Not Shown), 2. Thermistor Arrays, 3. Pressure Sensors, 4. Doppler Current Meter Located Approximately 50m South East of Tower Base	44

15.	View of Instruments as Seen Looking from West Elevation. 1. Wave Slope Sensor, 2. Thermistor Arrays, 3. Pressure Sensors, 4. Doppler Current Meter, 5(a). Wave Follower in Storage Position, (b) Wave Follower in Operating Position, 6. Wind Drag and Short Wave Slopes, 7. Stillwell Photography, 8. Surface Tension, 9. Stereophotography T-Bar, 10. Surface Tension, 11. (Not Shown), 12. C- to W- Band Multi-Band Frequency Radar	46
16.	RPI Surface Tension Measurement System	47
17.	View of Instruments as Seen Looking Downward at Catwalk Level. 1. Wave Slope Sensor, 2. Thermistor Arrays, 3-4. (Not Shown), 5. Wave Follower, 6. Wind Drag and Short Wave Slopes, 7. (Not Shown), 8. Surface Tension, 9(b). Stereophotography T-Bar, 10. Surface Tension, 11(c). Wave Gage Array	49
18.	View of Instruments Mounted as Seen from South Elevation. 1. Wave Slope Sensor, 2. Thermistor Arrays, 3. Pressure Sensors, 4. Doppler Current Meter, 5(a). (Not Shown), (b) Wave Follower in Operating Position, 6. Wind Drag and Short Wave Slopes, 7. Stillwell Photography, 8. Surface Tension, 9(a). Stereophotography, (b) Stereophotography T-Bar, 10. Surface Tension, 11(a). K_u - Band Radar, 11(b). K_u -Band Radar and 11(c). Wave Gage, 12. C- to W-Band Multi-Frequency Radar, 13. C-, k_a and G-Band Radar	50
19	13. C-, K_a - and G-Band Radar Instruments Mounted as Seen Looking Down from the Helicopter Deck Level.	52
20.	U.S. Coast Guard 25m Cutter Point Huron. One of Three Cutters will be made Available for Transportation to the Tower on a Noninterference Basis	55
21.	Rubber Raft Used by 25m Cutter to On/Off Load Personnel to and from the Chesapeake Light Tower. The 12m Cutters Can On/Off Load at this Tower Landing	56
22.	Organization Plan for SAXON I Experiment	57
23.	SAXON I Schedule of Events	58
24.	Data Management Center for the SAXON I Experiment	60

LIST OF TABLES

TABLE		PAGE
1.	Radar Frequencies and Wavelengths Proposed for SAXON I, and Investigated in Previous Experiments	8
2.	Aircraft Participating in SAXON I	10
3.	Matrix of SAXON I Science Objectives vs. the Planned Data Sets	11
4.	System Characteristics of C- and X-Band RAR On Board NRL RP-3A Aircraft	36
5.	System Characteristics of L-, C-, and X-Band SAR System on Board NACD RP-3A Aircraft . . .	39
6.	System Characteristics of the K_u Band Wave Spectrometer on Board the NRL RP-3A Aircraft .	41
7a.	Investigators and Corresponding Areas of Analysis	62
7b.	Investigators and Corresponding Areas of Analysis (Continued)	63

I. INTRODUCTION

SAR imaging of the ocean surface promises to be an important tool in ocean remote sensing. The long range goal of the proposed research is to understand SAR imaging in sufficient detail so that airborne and/or spaceborne SARs can become reliable tools for oceanic research, and for operational use.

The TOWARD Experiment provided a comprehensive data set that was required for verification of theoretical concepts on SAR imaging of the ocean surface. In the formulation of the experiment it was recognized that three distinct disciplines have to be addressed: (a) hydrodynamics, (b) radar backscatter and (c) SAR image processing.

A significant achievement from TOWARD is the determination that none of the then available theories on SAR imaging of long surface waves could explain all the SAR observations satisfactorily. Work is presently in progress to amend existing models. In addition, the following specific results were reported:

1. The probability density functions of wave slopes indicated Gaussian distribution for wave frequencies less than 2.5 Hz and non-Gaussian distribution for wave frequencies greater than 7.5 Hz. These distributions suggest that the longer ocean waves are weakly coupled, as expected, but that the very short surface waves are strongly coupled through possibly strong nonlinear interaction.
2. The measured wave slope spectra from the laser slope sensor and stereophotography in TOWARD indicated lower intensity levels compared to predictions by Pierson and Stacy (1973) and Donelan and Pierson (1985).
3. The radar backscatter results suggested that sea spikes do not contribute significantly to the average backscattered power at L-Band. Sea spike occurrence increased with radar frequency and wind speed.
4. The cross-wind radar backscatter results suggested that cross-wind or cross-wave modulation does occur, and constitutes a mechanism for SAR imaging of azimuthally traveling waves. The data also indicated that the radar backscatter spectrum had a small peak near the dominant frequency of long

waves, indicating a significant role for the velocity bunching mechanism.

5. SAR focusing results for azimuthally traveling waves indicated that waves have the highest contrast at a focus setting that is one order of magnitude greater than the wave orbital velocity. There is theoretical evidence that the range 0.5-1.0 times the phase velocity is the relevant magnitude.

The TOWARD results provide definitive conclusions regarding the physics of SAR imaging of the ocean surface. Indeed, because the TOWARD data sets provide the most complete surface-truth measurements in support of SAR today, it is anticipated that these data sets will be used for a number of specific scientific investigations related to SAR in the future. It is noted that the TOWARD data sets were directed at solving the L-Band SAR problem. A relatively small number of X-Band measurements were obtained at the same time to improve the basis for planning of future investigations on SAR imaging at higher frequencies such as SAXON I.

The achievement derived from understanding SAR imaging of surface waves at L-Band has an importance that transcends the immediate application of SAR detection of surface waves (although this application is important in itself). The most significant outcome of understanding SAR imaging mechanisms is the development of a theory for imaging the ocean surface that is consistent with observations. Understanding SAR imaging of surface waves at L-Band is a critical first step towards understanding SAR imaging of other ocean surface signatures. Hence, it is a natural follow-on from TOWARD to consider SAR imaging of internal waves, boundary currents and ship wakes, in various sea states and with multi-frequency radars.

SAR imaging of internal waves in the SARSEX experiment demonstrated that the observations at L-Band could be explained, to factors of 2-5, by the Bragg-resonant mechanism of the modulated surface waves. But the observations at X-Band could not be explained by Bragg only. The influence of intermediate surface waves was invoked, and shown to be crucial for explaining the observations. In SARSEX, it was implicitly assumed that simulated radar backscatter from the ocean surface is equivalent to variations in the SAR image intensity. This assumption is reasonable in low sea states, but not so in the higher sea states. In the latter situation, the orbital velocity field associated with surface waves induces a distortion in the mapping of the ocean surface to the SAR scene. The SAR

resolution is also degraded by surface motion effects, so that certain length scales on the ocean are eliminated in the SAR scene. The influence of surface waves on imaging internal waves is not well understood at present.

A limitation of the TOWARD experiment stems from the fact that the sea states encountered were low, and highly directed (due to the directional windows imposed by the Channel Islands). While the limitations allowed careful scrutiny of the SAR imaging theories, the need remains for testing such theories in higher sea states. To a limited extent, this need has been addressed in the LEWEX experiment where useful data sets have been acquired.

In summary, it can be stated that significant insights have been gained from TOWARD and SARSEX. Yet, gaps remain in understanding the SAR imaging processes. These are stated below:

1. Hydrodynamic interactions of very short waves (0.5-5 cm long) are strongly nonlinear and presently not understood.
2. Radar backscatter from short surface waves is influenced by the entire spectrum of surface waves with wave numbers smaller than the Bragg wavelength. The implied consequence is that modulation levels of long waves can increase with radar frequency. There is need for precise measurements and simulations, in an input-output sense, to demonstrate this potentially serious implication.
3. Radar backscatter measurements from the ocean surface exhibit spikes that increase with radar frequency and sea state. The available radar backscatter models have not explained these observations satisfactorily. Additional mechanisms due to specular, wedge and breaking wave effects must be considered.
4. SAR imaging of surface waves at X-Band and higher frequencies requires validation. There is also need for testing SAR imaging theories in high sea states.
5. There is a need for understanding the influence of sea state on imaging internal waves.

An important environmental factor in microwave remote sensing that is given emphasis under the Marine Microlayer program is the physio-chemical properties of the air-water

interface. This interface (marine microlayer) is different from the bulk water below and the atmosphere above it. It is a region where viscous forces are preeminent, where biogenic organic compounds form films, inducing wide ranging physio-chemical changes, and where the majority of ocean remote sensors image the sea surface. It is in this region that occurrences on molecular and micrometer scales influence air-sea coupling and interact with surface wave energetics which in turn modify the electromagnetic signal reflected or emanating from the sea surface. Thus, the technical issues which arise naturally from the available environmental data are:

1. What is the dynamic equation-of-state of the ocean's surface? How does the visco-elastic nature of the sea-surface change with time?
2. Is the surfactant concentration at a given place and time near a 2-D transition?
3. How do films originate? What is the residence time of surfactants at the surface of the ocean?
4. Is the ocean's interface a habitat for microorganisms? How do unique adaptations reveal biological and chemical succession at the interface?
5. What is the chemical composition of surfactant films? How does it vary oceanographically?
6. How do films affect interscale energy transfer of surface capillary and capillary-gravity waves?

The scientific objectives for SAXON I are carefully selected to include the above issues and are consistent with recommendations of the SAR Working Group report (1986). They are detailed in Section II.

The experimental approach for achieving the above goals is highlighted below:

1. Use a stable platform so that measurements of shortwaves and radar backscatter can be free of platform motion.
2. Provide simultaneous measurements of short surface waves, long surface waves, internal waves and relevant environmental parameters.
3. Provide for platform-based coherent and calibrated radar measurements in the frequency range 5-95 GHz

(corresponding to radar wavelengths of 0.3-6.0 cm). The aim is to relate these to amplitudes and slopes of surface waves so that: (a) the effect of the surface wave modulations on both SAR and RAR can be established, and (b) a radar confirmation of the modulation of short waves by long waves can be provided.

4. Obtain SAR and RAR digital images of the ocean surface with airborne radars at various azimuthal angles, height to velocity ratios, and environmental conditions; the emphasis is on 10 GHz radars.
5. Incorporate specialized systems for measuring surface tension, decay rate of short waves (Bobbing Buoy) and near surface wind speed.
6. The Chesapeake Light Tower is a stable platform, free from influence of land atmospheric influence. It is used in SAXON I to provide a host of specialized experiments.

II. SCIENTIFIC OBJECTIVES

The specific scientific objectives of SAXON I are:

1. Investigate the Hydrodynamic Modulation of Short Gravity and Capillary Waves (0.3-50cm) by Long Surface Waves (50-500m) and Internal Waves. Included in this Investigation is the Role of Intermediate Waves (0.5-50m).

There is now substantial evidence that short gravity waves 30 cm in length are better behaved hydrodynamically compared to 3.0 cm long waves. Hsiao and Shemdin (1983) report on this difference based on their MARSEN results. Hwang and Shemdin (1988) come to a similar conclusion based on Probability Density Functions (PDF) derived from the TOWARD laser slope data.

SAR images from the SARSEX experiment confirm that internal wave modulation levels at X-Band are similar in magnitude to those at L-Band. These observations can be explained by Bragg scatter modulations at L-Band but not so at X-Band. Two different analyses have been advanced to explain the X-Band observations. Both utilize multi-scale interactions. These are:

(a) X-Band Bragg waves are modulated hydrodynamically by intermediate scale surface waves which are in turn modulated hydrodynamically by the internal waves. This analysis is advanced by Watson (1986) and is primarily hydrodynamical in its approach.

(b) Internal waves modulate intermediate surface waves hydrodynamically. These modulated intermediate waves tilt the X-Band Bragg waves. The approach invokes a combination of radar backscatter and hydrodynamics. This analysis is discussed by Holiday (1986). The method is shown by Jang (1986) to be similar to a three-scale approach introduced in 1975 to explain the OWEX observations.

Considering the many assumptions invoked in both of the above approaches, it is seen desirable that a careful set of observations, involving short surface waves and radar backscatter, be acquired simultaneously to provide independent hydrodynamic and radar backscatter verifications to the SARSEX observations. Such measurements are also required for validating the hydrodynamic forcing functions, such as introduced by Hughes (1978), among others.

2. Determine Experimentally, using Tower-Based Systems, Radar Backscatter Modulations Induced by Internal Waves and Long Surface Waves, with Emphasis on Radar Frequencies in the Range 10-35 GHz.

The available evidence suggests that radar backscatter modulations, induced by internal waves, decrease with increasing radar frequency from P-Band to C-Band, then increase toward X-Band, presumably because of the intermediate surface wave effects discussed above. Considering that radar resolution and the number of independent samples increase with radar frequency, it can be determined that higher signal-to-noise ratios can be achieved at higher radar frequencies. The above suggests that radar frequencies higher than X-Band may yield larger modulations and higher signal-to-noise ratios compared to X-Band.

The OWEX data set covered the frequency range P- to K_a-Bands, as shown in Table 1. The TOWARD experiment covered the frequency range L- to Ku-Bands. It is planned here that the range L- to G-Bands be covered in SAXON I, with emphasis on X- to K_a-Bands. These measurements are crucial for determining the modulations induced by internal and/or surface waves at X-Band and higher frequencies. Both platform-based and aircraft deployed radar systems are to be utilized for this purpose.

The OWEX data set emphasized near grazing angles for the frequency range P- to K_a-Bands. In SAXON I, it is planned that measurements be obtained at incidence angles in the range 20°-60°, at frequencies similar to OWEX and extending upward to G-Band. The planned radar backscatter and in-situ short surface wave measurements allow testing of available radar backscatter models by using the in-situ data as input (into the simulation algorithms) and comparing the output with radar backscatter measurements. The measurements obtained in OWEX did not allow such validation. New mechanisms involving wedge and breaking wave effects, which were recognized after OWEX, will be explored in detail.

3. Test SAR Imaging Theories at X-Band and Higher Frequencies

The TOWARD data set has allowed resolution of long standing differences between the available SAR imaging theories. The theories that are being validated with the

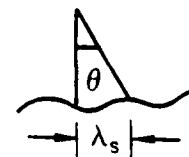
Table 1. Radar Frequencies and Wave Lengths Proposed for SAXON, and Investigated in Previous Experiments.

$$k_s = k_r \sin\theta$$

Surface Radar Incidence Angle

$$\lambda_s = \frac{\lambda_r}{2 \sin\theta} \quad (\text{Valid for Bragg})$$

$\theta = 0^\circ$	$\lambda_s \rightarrow \infty$
$\theta = 90^\circ$	$\lambda_s \rightarrow \lambda_r/2$
$\theta = 30^\circ$	$\lambda_s \rightarrow \lambda_r$



	Band	Freq	λ_r
	G	215 GHz	0.14 cm
	W	100 GHz	0.3 cm
	Ka	35 GHz	0.9 cm
	Ku	15 GHz	2.0 cm
	X	10 GHz	3.0 cm
	C	5 GHz	6.0 cm
	S	3 GHz	10.0 cm
	L	1 GHz	30.0 cm
	P	0.5 GHz	60.0 cm
		VHF	0.1 GHz = 100 MHz
	HF	10 MHz	30.0 m
	MF	2 MHz	150.0 m

TOWARD data will be further tested at X-Band and higher frequencies in SAXON I. It is proposed that equivalent resolution SAR and RAR images be obtained simultaneously in SAXON I over the instrumented site to enable such validation. As in TOWARD, surface observations will be used as input in the SAR simulations. The outputs will be compared with modulations derived from the actual images. The goal is to determine the skill of the SAR algorithms in determining the modulation levels and in estimating the degradation of SAR resolution. The simultaneous SAR/RAR images will be instrumental in achieving this objective. The aircraft participating in SAXON I are shown in Table 2.

4. Investigate the Influence of the Microlayer on Both Active and Passive Remote Sensing Techniques

The basic objective of the Marine Microlayer program of ONR is to understand the biological, chemical and physical processes controlling those properties of the ocean's surface responsible for textural variability imaged by microwave, visible and IR remote sensors. A two-pronged effort will be pursued as part of the Marine Microlayer program working in conjunction with the Ocean SAR program. In addition to the surface tension measurements taken at the Tower, a research vessel will operate in other coastal areas, e.g. off the U.S. West Coast.

In summary, four primary objectives are identified for the SAXON I experiment. These objectives are listed in tabular form, in relation to the data sets that are acquired, in Table 3. Here, the definition of subsurface hydrodynamics is shown separately because of its underlying importance in meeting the stated objectives. Table 3 shows that certain data sets are essential for all the SAXON I objectives.

It is emphasized here that the objectives stated above are intimately tied to the central goal of understanding the mechanisms responsible for SAR imaging of the ocean surface. Such understanding is prerequisite to establishing where and how the SAR can be used as an oceanographic research tool or for operational goals. The first of the above objectives allows understanding of the hydrodynamics associated with the ocean surface microstructure which the radar detects.

Table 2. Aircraft Participating in SAXON I.

Aircraft	<u>SAR Mode</u>			<u>RAR Mode</u>	
	L	C	X	C	X
NRL RP-3A				.	.
NADC RP-3A	.	.	.		

Table 3. Matrix of SAXON Science Objectives vs. the Planned Data Sets.

Data Sets	Objectives	Define Sub-surface Hydrodynamics	Investigate Hydrodynamics of Very Short Waves	Test Radar Backscatter Modulations	Test SAR/RAR Imaging Theories at High Frequencies	Investigate Micro-layer Influences
1	Laser Slope Sensor System-Short Waves
2	Stereo Photograph
3	Surface Tension
4	Directional Spectrum of Long Waves		.	.	.	
5	Meteorological Data
6	Thermistor Chains
7	Subsurface & Near-surface Current
8	Multi-Frequency Tower Radars	
9	C-Band SAR & RAR			.	.	.
10	X-Band SAR & RAR			.	.	.

The second objective investigates the link between the ocean surface and radar backscatter. The third objective allows determination of the effect of surface motion on the SAR imaging process, and the last provides needed information on how the surface microstructure can be enhanced or destroyed by natural surface films, which is frequently inferred to be the cause of certain strong modulations in SAR images.

III. THE FIELD SITE

A location off the U.S. East Coast, 22 km offshore Cape Henry, Virginia, known as the U.S. Coast Guard Chesapeake Light Tower (CLT), is selected as the field site for SAXON I, as shown in Figure 1. The following attributes are noted for the site:

1. It is the most suitable tower known as an alternative to the originally proposed field site, the OCNR Tower, San Diego, which was destroyed beyond repair in a major storm on 18 January, 1988.
2. The Chesapeake Light Tower is a rigid platform operated by the U.S. Coast Guard and is made available to SAXON I at no cost to ONR.
3. The Tower is located in 15m water depth, a location that is otherwise representative of open ocean conditions.
4. The site is free from wave refraction from nearby island effects.
5. Internal waves are generally present from April through October.
6. Swells propagate from the open ocean. Co-existence of swell and internal waves is a desirable environmental condition for addressing the SAXON I objectives.

The Chesapeake Light Tower is located 14 miles offshore of Cape Henry at $36^{\circ} 55' N$ and $75^{\circ} 43' W$. A recent photograph is shown in Figure 2. A side view of the Tower, as seen from the North, is shown in Figure 3. Platform elevations are marked in relation to the MLW level. A metal grating catwalk, shown in Figure 4, surrounds the Tower at the 5m level and provides a significant convenience for servicing many of the near surface instruments. The main deck has a grated platform at the 17m level. The quarter deck is at the 22m level and provides facilities for data gathering, computer systems and individual quarters. The 26m level is a helicopter deck, as shown in Figure 5. Helicopters can be used for transporting personnel and equipment to and from the tower. Facilities allow up to 20 scientists to operate during the day and remain on board during the night.

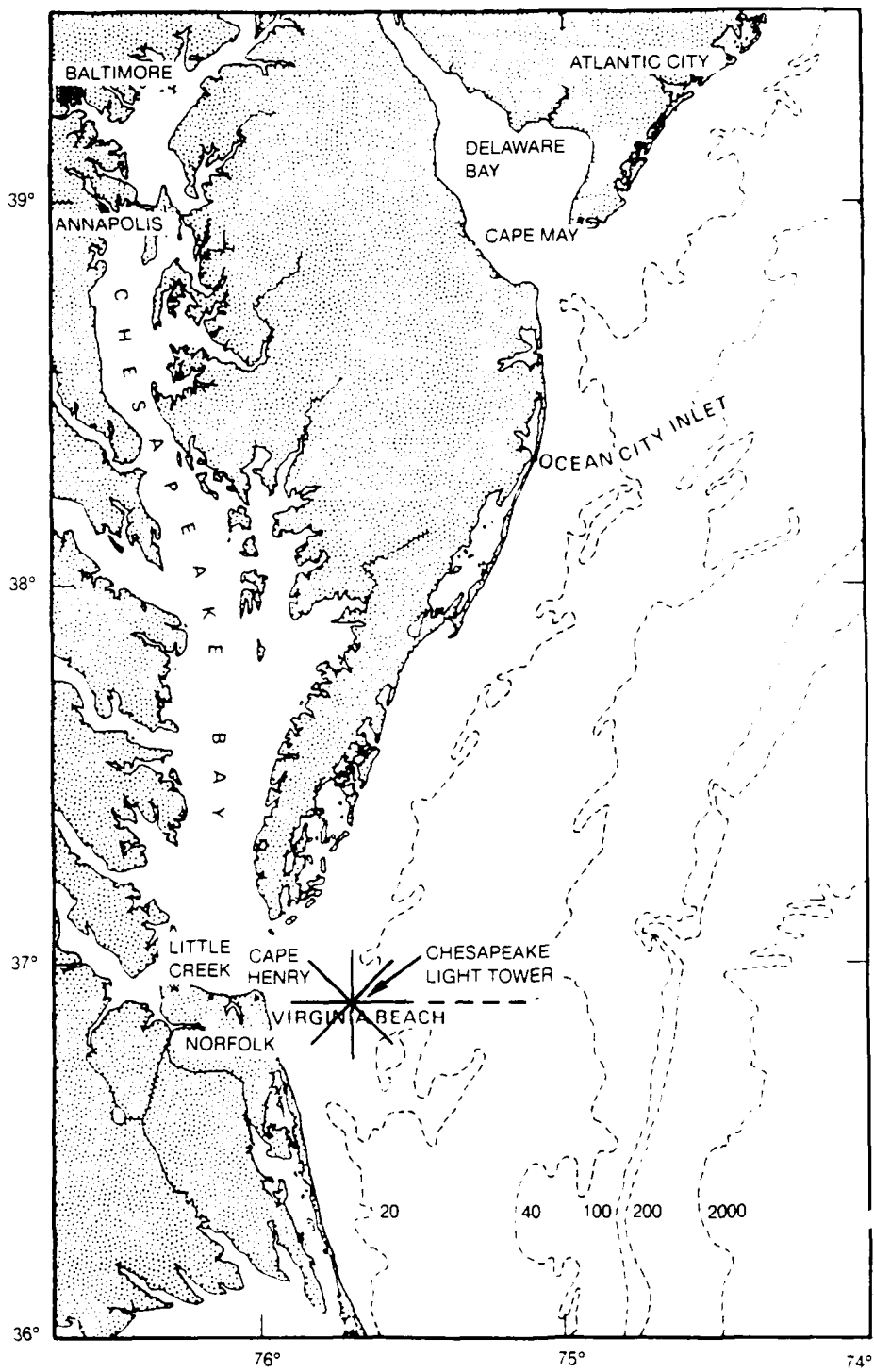


Figure 1. Location of Chesapeake Light Tower, Depth Contours in Meters. The Solid Lines Specify Nominal Flight Tracks Over the Tower.

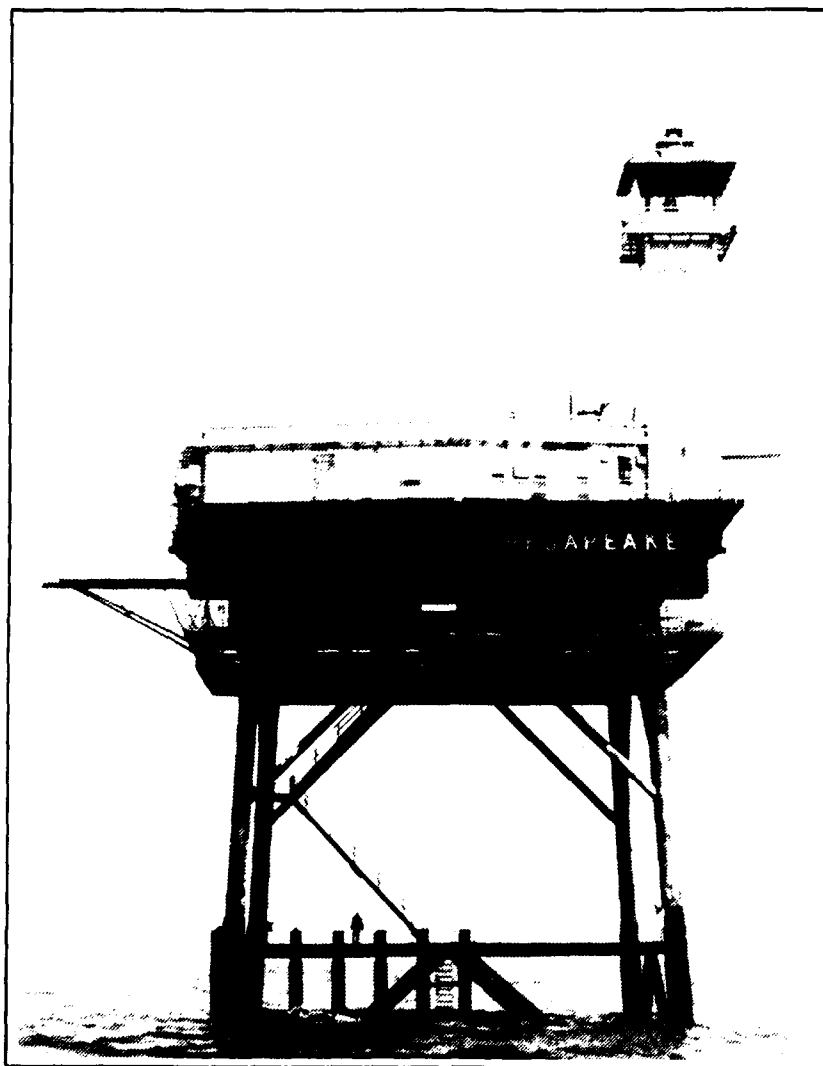


Figure 2. Recent Photograph of Chesapeake Light Tower as Seen from the South.

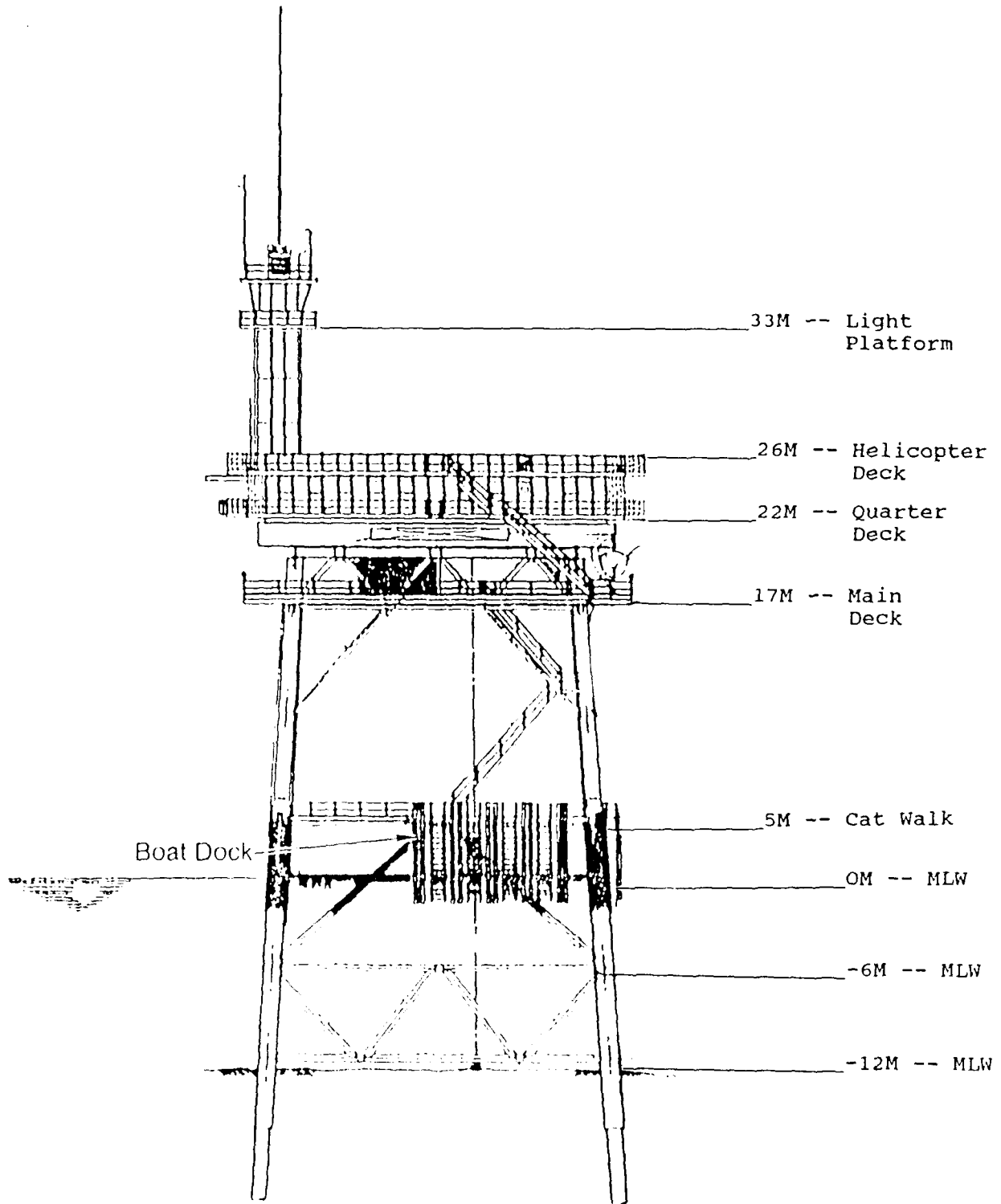


Figure 3. Side View of the Chesapeake Light Tower as Seen from the North Showing Elevation Levels. The Bottom is Now at - 15m.

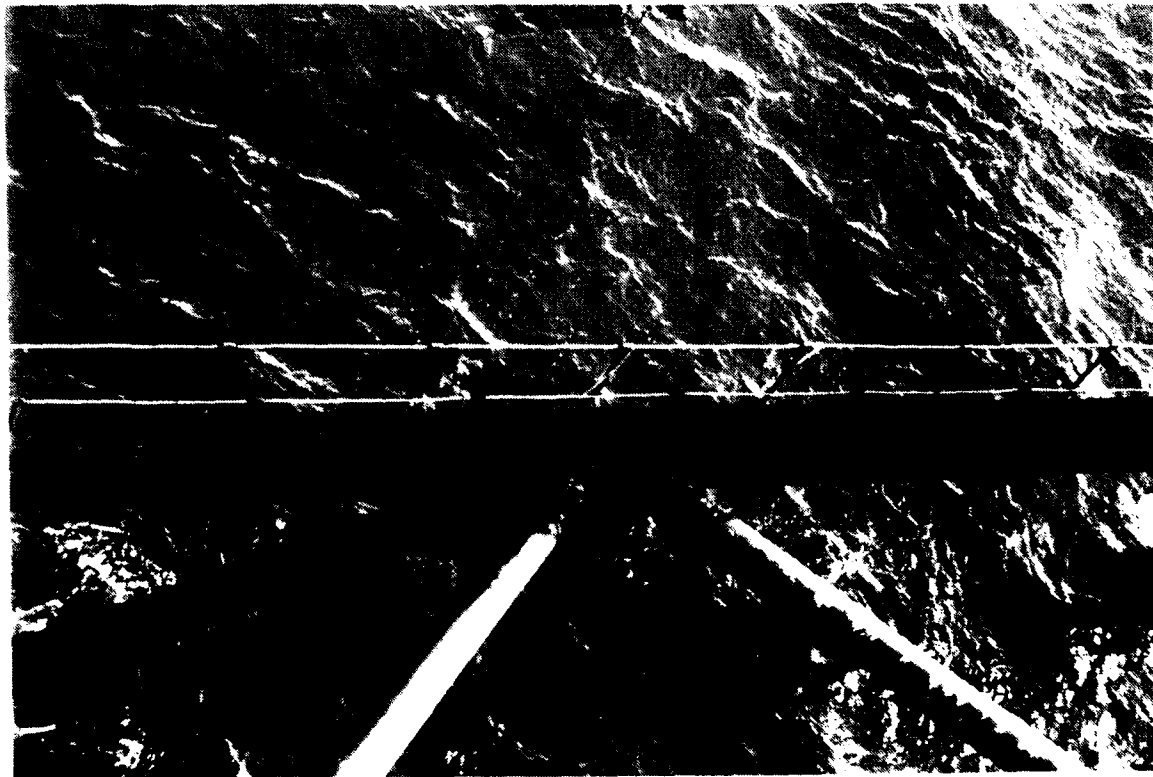


Figure 4. Catwalk Surrounding Chesapeake Tower at 5m Level Above MLW.

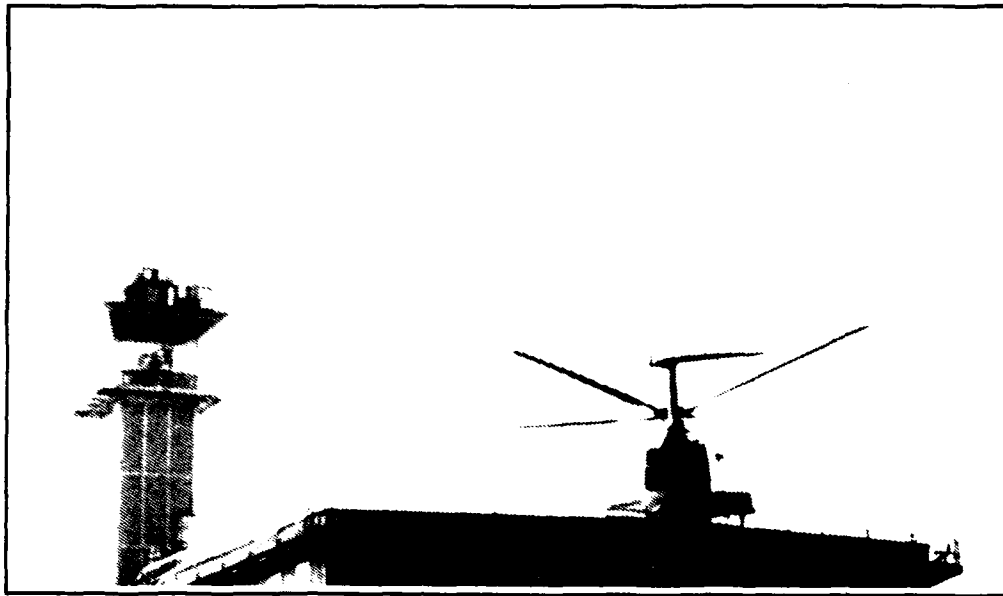


Figure 5. View of U.S. Coast Guard Helicopter Landing on the Helicopter Deck.

The environmental conditions in the Chesapeake region are summarized in a May 1984 report entitled "Wind and Wave Summaries for Selected U.S. Coast Guard Operating Areas" prepared by the U.S. Department of Commerce. Wind speeds, direction and frequency of occurrence for the months of July through December are extracted and shown in Figures 6 and 7. This represents information gathered from a location 30 km East of the tower site. During the month of September, winds are shown to be predominantly from the southwest ranging from 11 to 15 knots (5.7 to 7.8 m/s). Maximum winds of 42 knots (21.6 m/s) are a seldom occurrence. Similar conditions are reflective for the month of October with some variance of increased overall wind speeds, particularly above the 11-15 knot (5.7-7.7 m/s) range. During September to October, the wind direction is from direction west south west (WSW). Surface currents for August-September are 0.6 knots (0.3 m/s) from the north. The tidal range for this time period is 1.6m.

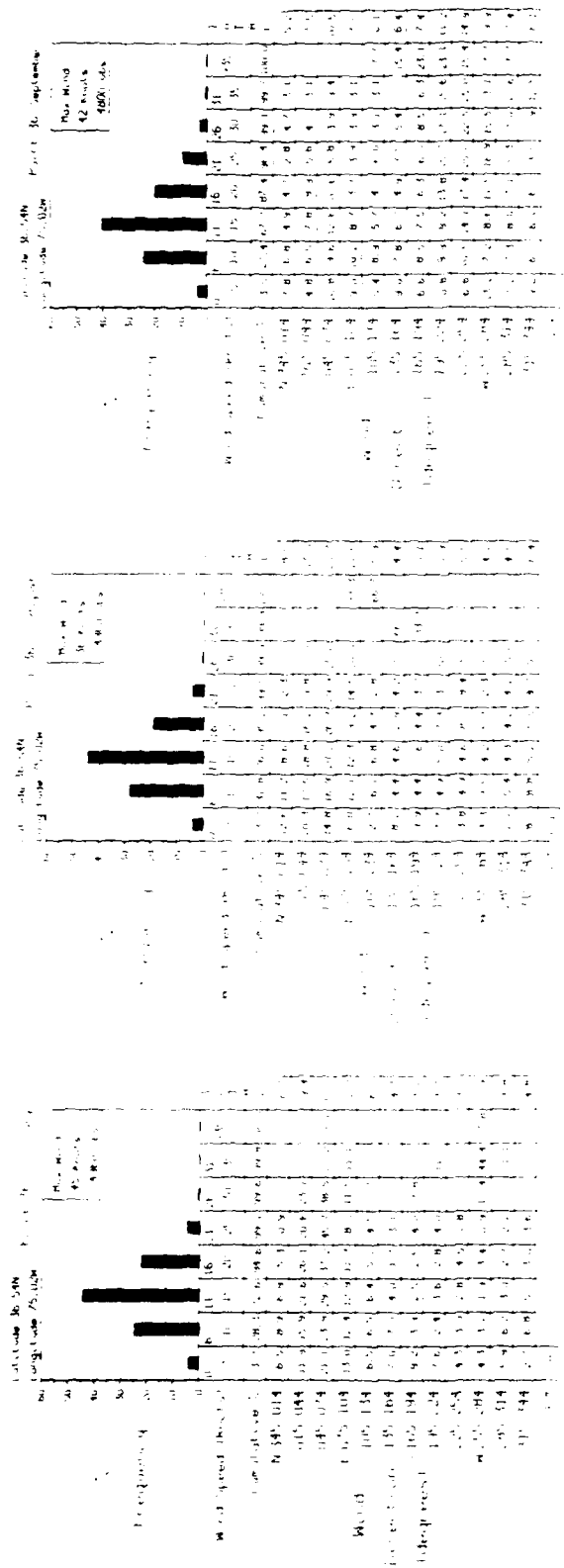


Figure 6. Surface Climatology in the Chesapeake Tower Vicinity as Provided by U.S. Coast Guard Wind and Wave Summary Report No. CC-D-05-84 for the Months of July - September.

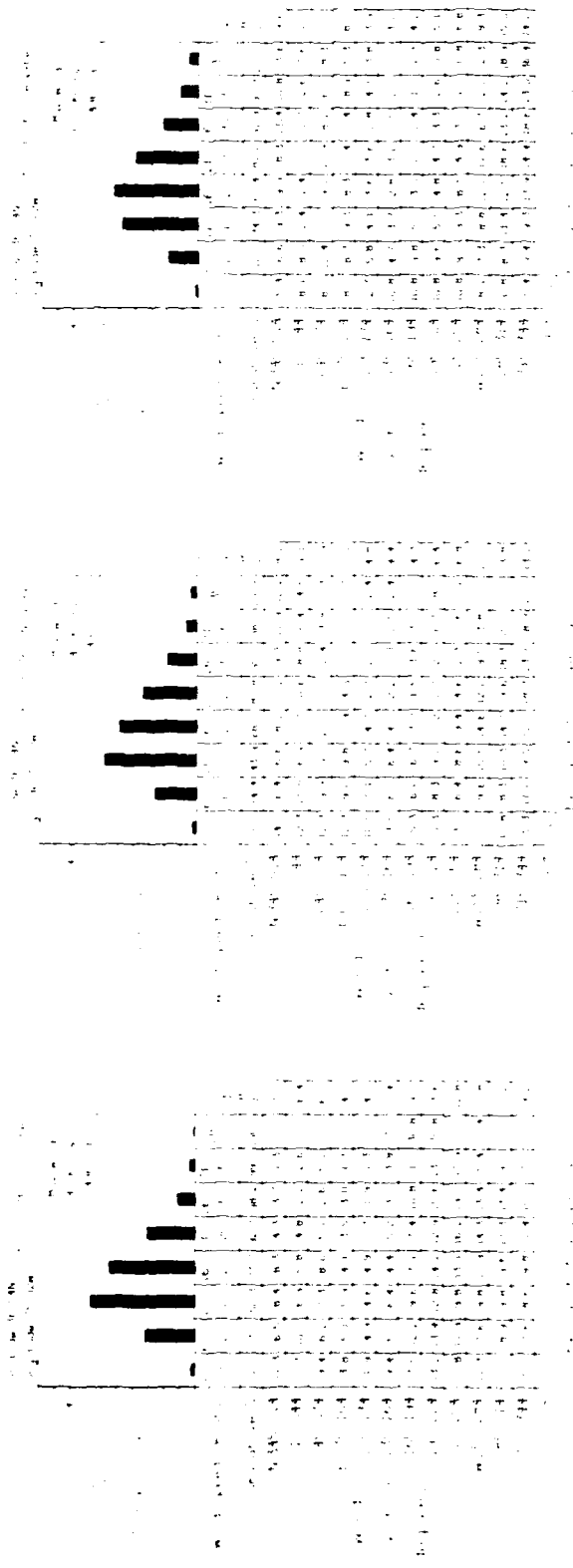


Figure 7. Surface Climatology in the Chesapeake Tower Vicinity as Provided by U.S. Coast Guard Wind and Wave Summary Report No. CC-D-05-84 for the Months of October - December.

IV. PARTICIPATION

The potential organizations, investigators and associated activities planned for the field operations phase of the experiment are shown below:

<u>Organization</u>	<u>Investigator</u>	<u>Investigation</u>
APL/JHU	B. Gotwols R. Sterner/ R. Chapman	Stillwell Photography
Case Western University	J. A. Mann/ J. Sanders E. Bock	Surface Tension Surface Tension Analysis
DTI	P. Jang/ S. Borchardt	Internal Wave Data Analysis
ERIM	A. Milman	Passive Microwave Radiometer
GSFC/NASA	T. Liu	Internal Wave Data Analysis
ISA	O. Lee	Internal Wave Measurements
JPL	R. Martin/ D. Hoff/ R. Steinbacher	Wave Follower Instrument Design and Operation
La Jolla Institute	F. Henyey/ J. Wright R. Daschen M.S. Longuet-Higgins	Hydrodynamic and SAR Modeling Nonlinear Hydrodynamics Theory
MIT	K. Melville/ A. Jessup	Breaking Waves and Backscatter Looking at Nadir

MPL	K. Watson	Hydrodynamic Modulation Theory
	P. Hanson/ S. Beck/ P. Jordan	Tower Support
NADC	A. Ochadlick/ H. Kritikos/ J. Lee	L, C-, and X-Band SAR
NORDA	P. Smith	Surface Waves Buoy
NOSC	J. Rohr	Acoustic Measurements
NPGS	K. Davidson	Wind Stress Measurements
	E. Thornton/ T. Stanton	Doppler Acoustic Measurements
NRL	G. Geernaert	Atmospheric Turbu- lence, Drag and Stability Measurements
	W. Keller/ P. Richardson W. Plant	C-Band RAR Measurements C- and K _u -Band Tower Radar
	D. Schuler	
	W. Barger	Surface Film Observations and Characterizations Passive Radiometer (SSM/I) Measurements
	G. Sandlin/ J. Hollinger/ A. Rose	
ORE	P. Hwang/ C. Palm	Short Surface Wave Slope Measurements and Analysis
	D. Hayt	SAR/RAR Data Processing
	D. Kasilingam	SAR/RAR Theory and Simulation
	M. Tran	Stereophotography

ORINCON	W. Garrett	Measurement, Analysis, and Modification of Surface Slicks and Surface Compressi- bility
RPI	J. Korenowski/ B. Asher	Surface Tension Measurements
SIO	R. Guza/ M. Clifton	Directional Long Wave Measurements, Ambient Tower Measurements
UCSD	R. Daschen	Radar and Hydro- dynamic theory
U. Delaware	D. Lyzenga	SAR Theory
U Kansas	R. Moore/ J. West/ P. Gogineni/ J. Holtzman	5, 10, 15, 35 and 95 GHz Tower Radar Measurements
U Mass	C. Swift/ R. McIntosh/ I. Popstefanija	5, 35 and 200 GHz Tower Radar Measurements
U Texas A&M Arlington	A. Fung	Radar Backscatter Modeling
U.S. Coast Guard	D. Paskausky/ J. Abbott/ P. Pallo/ C. Parks/ J. Brown/ J. Armquest	Tower Support
USGS	S. Wu	Stereo-Processing

V. FIELD MEASUREMENTS

The experimental resources proposed for SAXON I are outlined below:

A. Chesapeake Light Tower

The Chesapeake Light Tower is a stable platform located 22 km offshore of Cape Henry. The wave follower mechanism is mounted on the south side of the tower structure. An endless cable system, shown in Figure 8, allows the instrument frame to be moved vertically so it maintains a constant submergence depth as it rides on the long ocean waves (Shemdin, 1966 and 1980, and Hsiao and Shemdin, 1983). The vertical motion of the instrument frame is controlled by a wave gage which provides the signal to the servo-motor.

The following measurements are incorporated at the tower site:

1. Directional Spectra of Short Surface Waves

Short surface waves are measured by three independent techniques. The first uses a laser-optical system that measures directional wave properties. The second technique utilizes stereophotography to measure directly the two-dimensional wave number spectra of short surface waves. The third uses the familiar Stillwell photography which is known to be dependent on sky-brightness. These techniques are described briefly below.

a) Laser-Optical System - The ocean-going wave slope instrument used in TOWARD is modified so that space-time variabilities of surface waves can be measured. Figure 9 shows a sketch of the laser beam acceptance cone of the optical receiver portion of the wave slope instrument for two different maximum wave slope measurement capabilities. The 25.49 degree acceptance cone is associated with a 45 degree wave slope; the 7.12 degree acceptance cone is associated with a 20 degree wave slope. It is seen here that a portion of the optical receiver is unused for sea state conditions which produce smaller maximum wave slopes. The wave slope instrument is designed to be insensitive to where the laser beam enters the optical receiver; it simply measures the laser beam deflection angle, regardless of the beam's entry location. The unused portion of the optical receiver acceptance cone is therefore available for spatial scanning purposes.

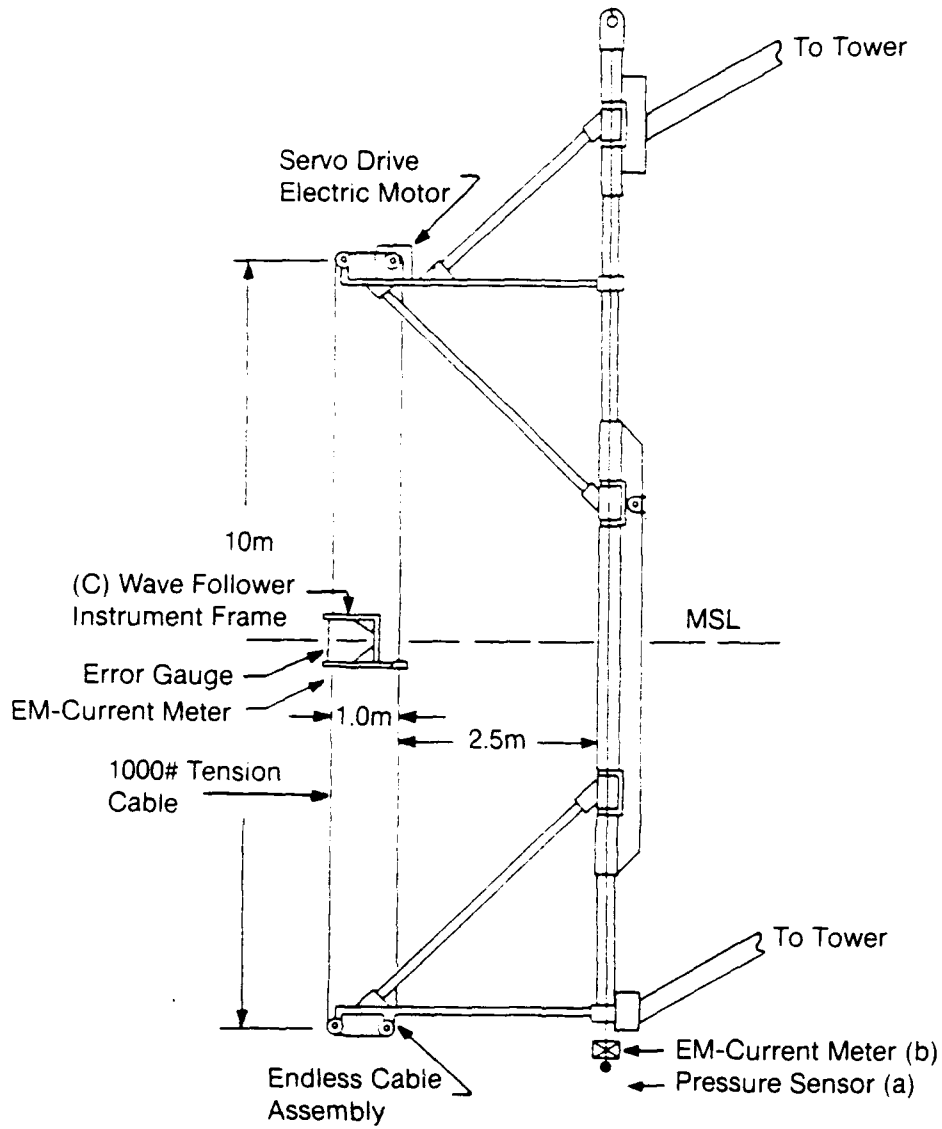


Figure 8. Wave Follower System in Operation with the Wave Slope Sensor.

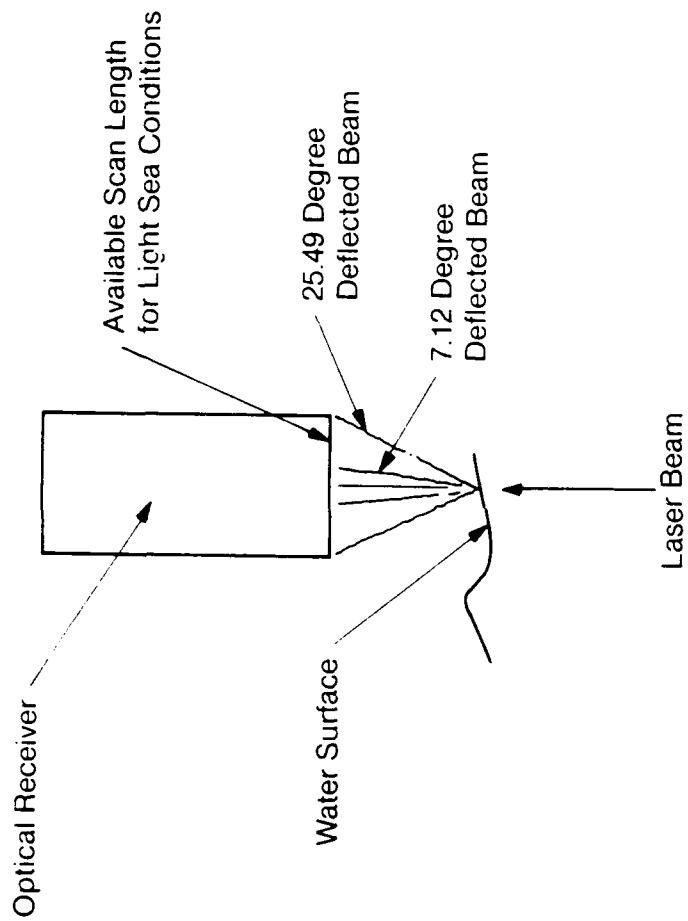


Figure 9. A Sketch of Laser Beam Acceptance Cones.

b) Stereophotography - For short surface waves stereophotography has an advantage over Stillwell type photographic analysis in that the directional spectra of the ocean surface are not sensitive to sky brightness variation or sun angle. The directional spectra obtained by stereophotography are an order of magnitude more accurate and can extend to a higher range of wave numbers where the amplitudes are typically very small. This requirement is consistent with the need to resolve Bragg waves of order 1.0 cm in order to compare with 35 GHz radar measurements. Stereophotographic analysis from the TOWARD experiment has clearly demonstrated the feasibility of this technique. A schematic of typical tower stereo-geometry is shown in Figure 10. An automated high-speed stereo-system is used in SAXON I.

c) Stillwell Photography - Although stereophotography has some distinct advantages, the Stillwell technique is faster, more economical, and of considerable importance; it provides a means for comparison with the stereo-derived wave number spectra. The Stillwell photography consists of the use of one or more video cameras that have high or low resolutions. This technique is sunlight dependent, and the mounting location of the cameras is crucial in that the sun must be behind the cameras. Clouds are a problem in that they cause changes in the brightness of the images. Clear weather is preferred. The cameras must be positioned as high above the surface of the ocean as possible, usually 8-9 meters with 10-11 meters most desirable. The cameras are operated in the look direction of SAR. The information is recorded on video tape, and analyzed subsequently in the laboratory.

2. Directional Spectra of Long Surface Waves

The measuring system consists of an array of pressure sensors mounted on the bottom and on the tower frame. Although high resolution directional ($\pm 10^\circ$) wave height spectra are desired in support of radar observations the system to be deployed in SAXON I will have directional resolution of order $\pm 25^\circ$. Only waves with frequencies less than 0.3 Hz will be measured with this array. The object is to obtain frequency and directional spectra for comparison with radar images. The measurements also allow the determination of the nonlinear distortions in the wave dispersion relationship.

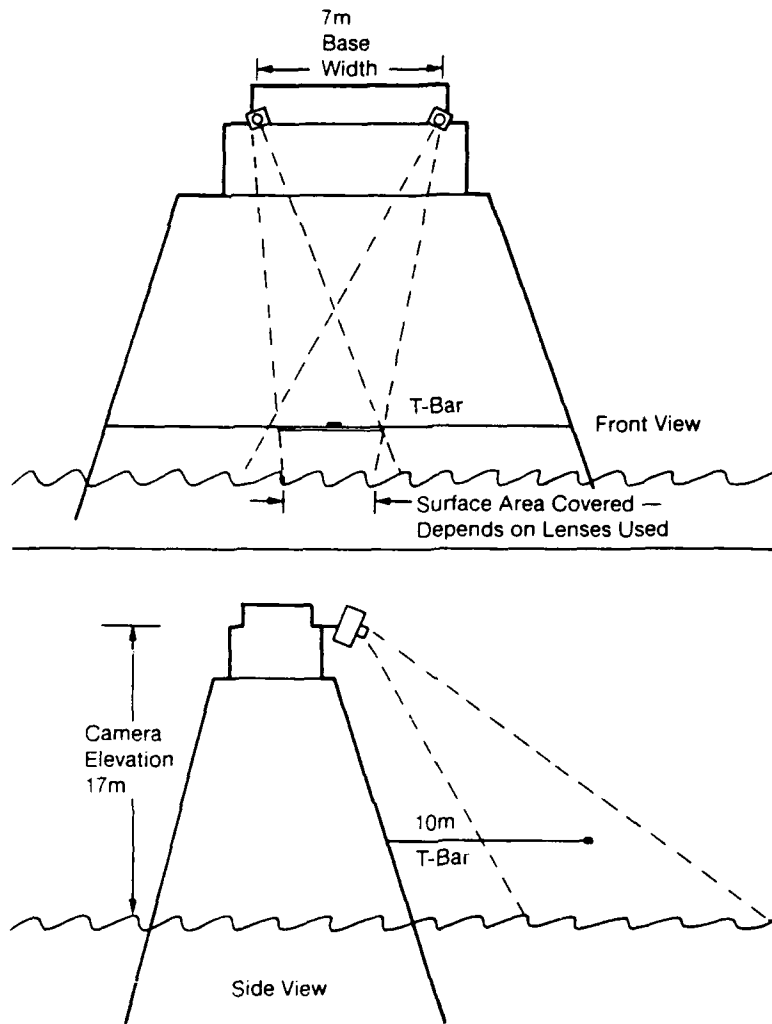


Figure 10. Schematic of Stereo-Geometry. The Cameras Show the T-Bar in Their Field of View for Calibration.

3. Directional Spectra of Internal Waves

Internal wave measurements are obtained at the tower with an array of thermistor chains. Four 28-element thermistor chain arrays are deployed to insure measurement of space-time variability of internal waves. These are suspended by strain members positioned at each leg of the tower. Each thermistor chain will have 28 thermistors calibrated according to pre-determined specifications.

4. Microlayer

In collaboration with ONR's Microlayer Accelerated Research Initiative program, several techniques for measuring surface tension, compressibility and other microlayer properties are deployed to obtain these properties simultaneously with other surface measurements. One of these techniques is deployed on board the wave following C-frame so that microlayer properties and short wave slopes can be obtained simultaneously in the proximity of the same ocean surface patch. Other microlayer techniques are deployed at a different location on the tower.

5. Ambient Measurements

Measurements of the wind stress (via both sonic and dissipation systems on the tower, and dissipation technique on a nearby buoy), wind speed and direction, atmospheric stratification (heat flux), air and water temperatures, wave height, tide level, near surface currents (using Doppler acoustic sensors), and surface tension are obtained. All these quantities are routinely recorded during the intensive measurement periods of SAXON I. The data will be distributed to all investigators as background information to support the analyses.

6. Tower Mounted Radar Systems

Two multi-frequency and one single frequency radar systems are deployed on the tower, as detailed below:

a) University of Kansas Multi-Frequency (C- to W-Band) Radar - These are broadband FM tracking radar scatterometers. One system covers 5, 10, and 15 GHz frequencies, and two other systems operate at 35 and 94 GHz. Use of excess sweep bandwidth allows averaging more independent samples for each measurement than would otherwise be possible, thereby reducing the degradation of measurement precision by fading. Separate antennas are used for vertical and horizontal polarizations at the three lower

frequencies. Beamwidths of the antennas range from 2.5 deg to 6 deg. The antennas are mounted together so that all may be pointed at the same spot on the surface. These systems track the slant range by automatically adjusting the sweep duration, which is measured. This allows measurement of the surface elevation at the centroid of the beam, thereby permitting direct computation of the cross-spectrum of the wave height and radar signal strength for studies of the modulation of the radar signal and the ripples by the long waves.

A vector slope gage is used for the first time during SAXON I. This system uses three 35-GHz ranging radars with narrow beams pointed to different spots within the wider beam of the lower-frequency system. The heights of the three spots can be used to determine orthogonal components of the local surface slope within the wider radar beam. This permits determination of the true slope modulation of the radar signal so that slope and hydrodynamic modulations can be separated.

A video camera is used to monitor the scatterometer beam location to assist in identifying causes of sea spikes.

b) University of Massachusetts Radar Systems - This system has three radars that are used on the tower. They are C-, K_a - and G-Bands with frequencies corresponding to 5, 35, and 215 GHz, respectively. The beam widths of the K_a - and the G-Band system is operated in FMCW mode to measure radar cross-section, but is now modified to obtain, in addition, Doppler information. The University of Massachusetts data acquisition system is able to handle data from all three radar systems, simultaneously.

c) NRL K_u -Band Radar System - Two K_u - Band (14 GHz) coherent Doppler scatterometers with dual linear polarizations are used on the tower. One is mounted at a vertical incidence on a 7.5 m horizontal boom along with a Thorn IR wave height sensor. This scatterometer has a 5 degree two-way half-power beamwidth. The second scatterometer has a 2.52 degree two way, half power beamwidth. It is mounted at a 45 degree incidence angle along with a video camera. The azimuthal angles depend on wind and wave directions.

A wave gage array with one decimeter spacing is located near the illuminated area.

d) NRL Passive Microwave Radiometers - NRL participates in SAXON I with their SSM/I - simulator radiometers tuned to frequencies 19GHz, 22GHz, 37GHz and 85.5GHz (the SSM/I passive microwave imager is deployed aboard the DMSP satellite). The radiometers are operated during the periods of DMSP overflights. Also the NRL radiometers are operated in parallel with the NPGS wind stress sensors to determine the correlation between the two techniques in measuring surface wind stress. Particular emphasis is devoted to the passage of meteorological fronts. Additional emphasis is given to the detection of surface films, and sea surface variation induced by ship wakes.

B. In-Situ Measurements in Proximity of Chesapeake Light Tower

The in-situ measurements in proximity of the Chesapeake Light Tower include the following:

1. Capacitance Wave Probe Spar Buoy

A schematic of the buoy is shown in Figure 11. The spar buoy is 9 cm in diameter and 6m in length. The suite of instruments mounted on the spar include an array of six capacitance surface elevation probes, a compass, an accelerometer, and an anemometer. The buoy is equipped with a vane which generally moves down-wind, keeping the array of wires up wind of the buoy. The compass provides an estimate of the wind direction. Data is logged on board the buoy in a Sea Data digitizing data logger. The resonant frequency of the spar (in vertical motion) is approximately 10 seconds. The buoy is designed to "follow" swell with period 10 seconds or longer. The accelerometer is included to record the omni-directional height of the low frequency swell component.

The array of capacitance wires is spaced at distances appropriate to the segment of the wave number spectrum for which an estimate of the directional spectrum is desired. The array is scanned at 32 Hz, and pre-filtered at 15 Hz to avoid aliasing. For SAXON I, the sensor wire is replaced by a resin-coated piano wire with the working section being 170 cm long.

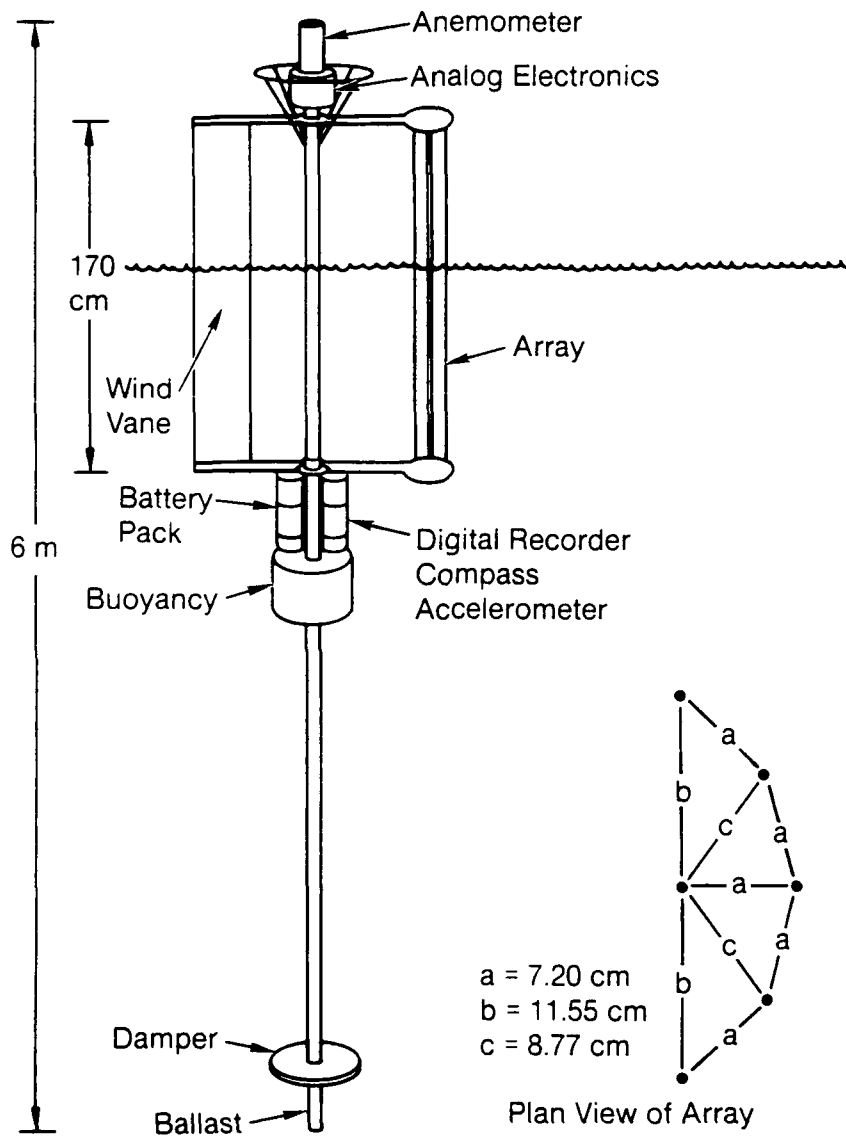


Figure 11. Capacitance Wave Probe Spar Buoy.

The mode of operation is to deploy the buoy from a ship for a period of from 25 to 30 minutes, using the ambient current or wind to advect it through the area of interest. The buoy is then brought back aboard the deploying vessel, and the 1 megabyte memory dumped to the shipboard computer while the batteries are re-charged. This process takes about 25 minutes after which the buoy is re-deployed.

The data provides estimates of frequency directional spectra and wave slope statistics as a function of the buoy position averaged over the appropriate time interval. Slope statistics are obtained by producing a time-dependent estimate of the wave slope, spatially averaged over the area subtended by the area of the array. This is accomplished by fitting the best flat facet through the elevation data. The slope distribution obtained in this way, from data collected at Nantucket Shoals, shows an extremely directional nature to the distribution, for wavelengths of 15 cm or greater.

Directional spectra are derived from a least squares fit of the cross spectra of the wire data with a model, using an expansion of the wave field in circular harmonics.

2. Wind Stress Buoy - This buoy is deployed off the Chesapeake Light Tower to evaluate tower measured stress results, and to relate the momentum flux co-spectra (sonic anemometer) to the direction of the surface stress vector under different vector wind and wave conditions. The measurements are designed to correlate surface layer wind velocity and wind stress with scatterometer and SAR signatures.

3. Acoustic Measurement - The effect of monomolecular films on acoustic measurements will be determined. Although measurements of the damping of ocean surface waves by nonmolecular films, using wave staffs and microwave radar, is not new, those measurements combined with acoustic measurements are. Besides allowing for a generally much better correlation between ocean roughness and ambient noise, there is an opportunity to determine the following:

a. The threshold of ocean surface roughness when the film's effects become first noticeable. Previous measurements at very low sea states indicate that the film does not have an effect.

b. At higher sea states, it is observed that different films have nonidentical effects on the higher frequency ambient noise. An effort will be made to determine if this is associated with similar effects on bubbles.

c. The acoustic effects of the slick are unsteady. At the lower sea states, the film's effect can persist for 1-2 hours; it is not clear if this is a consequence of the film drifting past the hydrophone or of the film breaking up. An attempt at such evaluation will be made.

d. In the event of extremely high sea state, it is of interest to determine if the films can significantly reduce white capping.

Two sonobuoys are to be deployed near the tower approximately one or two kilometers apart. Ambient noise levels are recorded at the tower and compared simultaneously. One of the sonobuoys is placed within a footprint where surface roughness measurements are obtained before and after the film is deployed. In-situ measurements of wind speed, current and sound velocity profiles are collected simultaneously with the acoustic measurements.

C. Airborne Measurement Systems

The airborne radar systems that are participating in SAXON I are shown in Table 2. Here, both systems are briefly discussed and the radar characteristics given.

1. C- and X-Band RAR on Board NRL RP-3A

The Naval Research Laboratory has developed a real aperture radar (RAR) for the purpose of producing images of backscatter from the ocean surface in terms of radiometrically correct normalized radar cross sections (NRCS). The system characteristics are given in Table 4. The system is flown on NRL's RP-3A aircraft and is to operate at both X- and C-Bands. It is developed for the primary purpose of co-flying with a synthetic aperture radar (SAR) in order to examine and understand differences in ocean imagery between the two systems. The RAR records its data in a digital format directly on disc to facilitate the production of images of absolutely-calibrated NRCS values. A coherent pulse-to-pulse integration is incorporated to improve signal to noise ratios, while subsequent averaging of detected signals produce statistically stable NRCS values. Presently planned operating procedures call for the production, not of continuous imagery, but of imagery of a finite area (probably of dimensions 2 to 4 km by 1 to 10 km) followed by a gap while data are being stored.

Five RAR flights are scheduled during the SAXON I experiment. An eight-sided flight pattern, shown in Figure 12, is to be flown in a manner identical to that flown by the SAR aircraft (see 2, below). The RAR system is flown

Table 4. System Characteristics of C-, and X-Band RAR System On Board NRL RP-3A Aircraft.

	X-Band	C-Band
Center Frequency (GHz)	9.375	5.30
Wavelength (cm)	3.0	6.0
Pulse Length (μ sec)	100	60
Bandwidth (MHz)	---	---
Peak Power (kW)	10	10
Antenna Azimuth Beam Width (deg)	0.9	1.5
Antenna Range Beam Width (deg)	23	---
Antenna Beam Center Gain (dB)	45	45
Nominal Altitude (km)	0.3-3.0	0.5-2.0
Nominal Ground Speed (m/s)	180	180
Flight Duration (hrs)	12	12
Nominal PRF (pps/pol) at 257 m/s	0.77 x alt	2.83 x alt
Swath Width (km)	0.24 - 2.4	---
Resolution		
Slant Range (m) x Azimuth (m) - Digital	20 x 0.02 altitude	7.8-30 x 13.6-200
Incident Angle	45	
Polarization	HH	HH, VV

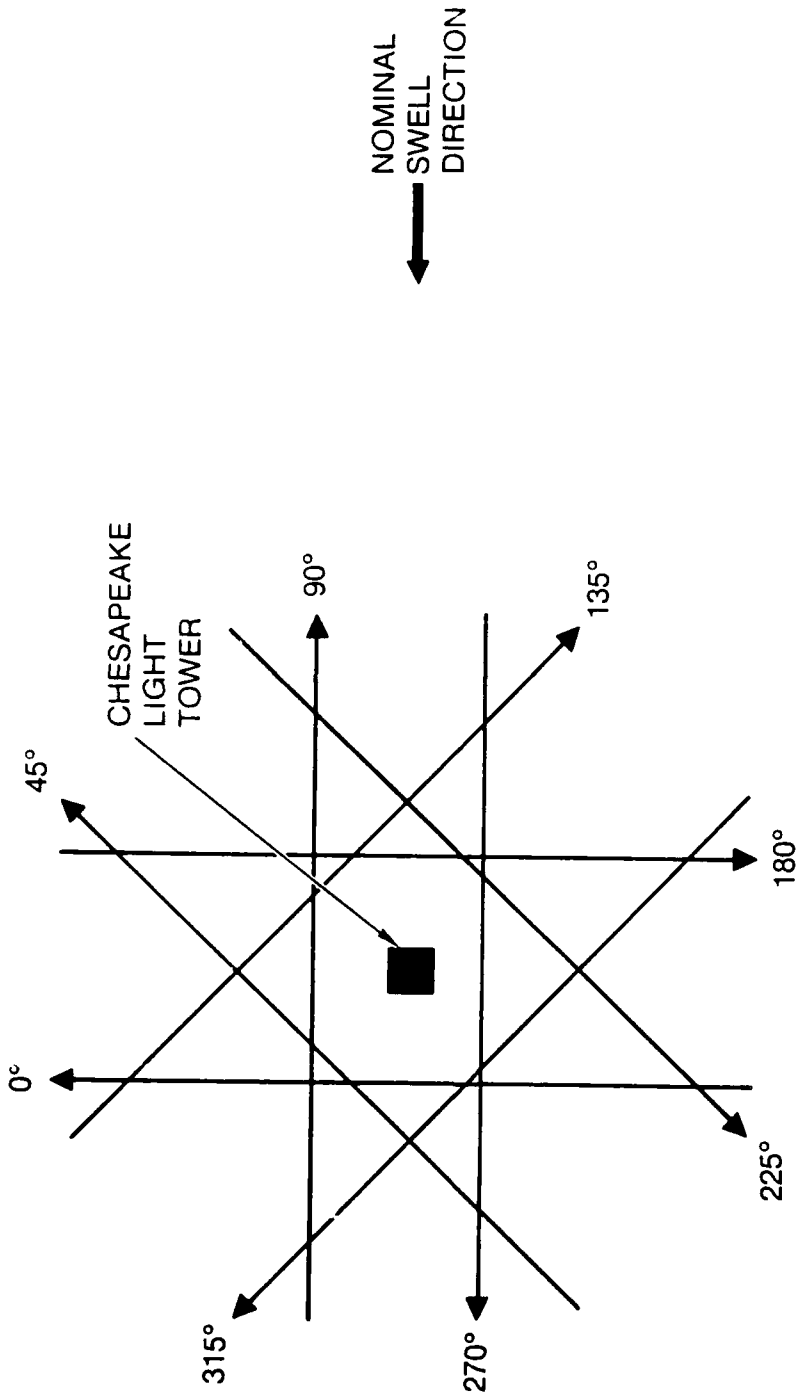


Figure 12 Flight Patterns for SAR and RAR.

only at 915 m elevation. The pattern is rotated with respect to the direction of surface waves or internal waves.

2. L-, C- and X-Band SAR on Board NADC RP-3A

A multifrequency-polarimetric SAR is constructed for remote sensing applications. There are many applications of multifrequency-polarimetric SARs. These use the polarimetric channels to extract geophysical information as well as to gain insight into the backscatter mechanism. This SAR operates at a range resolution of 2.4m and an azimuth resolution of 2.2m in the fine resolution mode, and at twice the range resolution in the course resolution mode. This new SAR is installed in an NADC RP-3A aircraft which is modified for research and development use. The system characteristics are shown in Table 5. Three frequencies are used, L, C, and X-Band. All of the elements of the polarization matrix are collected at each of the frequencies. The data is recorded in several forms. High density digital tape (HDDT) is used as the primary recording medium. Data is recorded on photographic film for subsequent processing and a real-time image formation processor records image data on heat-developed paper. Four channels of HDDT are available, each capable of rendering 4096 range elements.

Five SAR flights are scheduled during the SAXON I experiment. These are executed in an eight-sided pattern centered around the tower, as shown in Figure 12. The same pattern is flown at three different altitudes (1,525 , 3,049 and 7,012 m), consecutively. The pattern is rotated depending on swell or internal wave direction.

The flight duration consists of five minute runs, each 3.0 km long, with headings 0, 45, 90, 135, 180, 225, 270, and 315 when the nominal swell or internal wave direction is from the East. The estimated flight time for one eight-sided pattern is 80 minutes. The estimated flight time over the tower is four hours. Allowing for two hours in transit the estimated mission duration is six hours.

The SAR system is equipped with four channels of recording, hence allowing simultaneous recordings of one frequency at four polarizations, or three frequencies at one polarization. The emphasis in SAXON I is on simultaneous measurements at different frequencies. Calibrated radar measurements obtained with this system will be compared with equivalent RAR measurements under similar environmental conditions. Both aircraft systems are calibrated using corner reflectors placed at the Patuxent River Naval Air Station.

Table 5. System Characteristics of L-, C-, and X-Band SAR System On Board NADC RP-3A Aircraft.

	<u>L-Band</u>	<u>C-Band</u>	<u>X-Band</u>
Center Frequency (GHz)	1.25	5.26	9.3756
Wavelength (cm)	24	5.7	3.2
Pulse Length (μ sec)	4.0	4.0	4.0
Bandwidth (MHz)	—	—	—
Peak Power (kW)	5.0	1.4	1.5
Antenna Azimuth Beam Width (deg)	10.0	2.2	1.25
Antenna Range Beam Width (deg)	—	—	—
Antenna Beam Center Gain (dB)	—	—	—
Nominal Altitude (km)	7.6	7.6	7.6
Nominal Ground Speed (m/s)	180	180	180
Flight Duration (hrs)	12	12	12
Nominal PRF (pps/pol) at 250 m/s	2200/4400	—	—
Swath Width - Quad Pol Mode (km)	—	—	—
Resolution (4 Looks)			
Slant Range(m) x Azimuth(m)-Digital	1.6 x.2.2	1.6 x.2.2	1.6 x.2.2
Incident Angle	—	—	—
Polarization	HH, VV, HV, VH	HH, VV, HV, VH	HH, VV, HV, VH
Linear Dynamic Range - Power			

3. K_u-Band Wave Spectrometer On Board the NRL P-3

A three-Frequency K_u-Band scatterometer, designed to make directional measurements of ocean wave spectra is flown aboard the NRL RP-3A aircraft. This system is the implementation of a new concept and is capable of measuring ocean wave slope spectra with 15 degree azimuthal resolution. Data from the system recorded in a digital format directly on discs. Data processing is well developed and preliminary spectra become available just after each flight. Measurements are (typically) made on ocean wavelengths between 5 and 200m. This radar is simultaneously used as a calibrated K_u-Band scatterometer measuring σ_0 . Estimates of surface wind speed and direction are produced from this data. The characteristics of this Ku-Band system is shown in Table 6.

D. Ship Wakes

Consistent with the objectives of the SAXON I experiment, several ship passes are scheduled during the period 19 September to 14 October. A schematic of a typical ship pass is shown in Figure 13. Simultaneous SAR and RAR images of the ship wakes are scheduled during the various passes. Also, continuous backscatter and in-situ capillary wave measurements are scheduled during the periods when the turbulent and Kelvin wakes drift past the tower.

Table 6. System Characteristics of the K_u Band Wave Spectrometer On Board the NRL RP-3A Aircraft.

Center Frequency (GHz)	14.0
Wavelength (cm)	2.01
Pulse Length (μ s)	1-10
Peak Power (W)	10
Antenna Beamwidth (Deg.)	4.5 x 4.5
Nominal Altitude (km)	3.05
Nominal Ground Speed (m/s)	103
Polarization	VV
Range of Incidence Angles (Degrees)	5-55
Number of Independent Averages/Measurement	96
Along track extent of measurements (km)	5.2

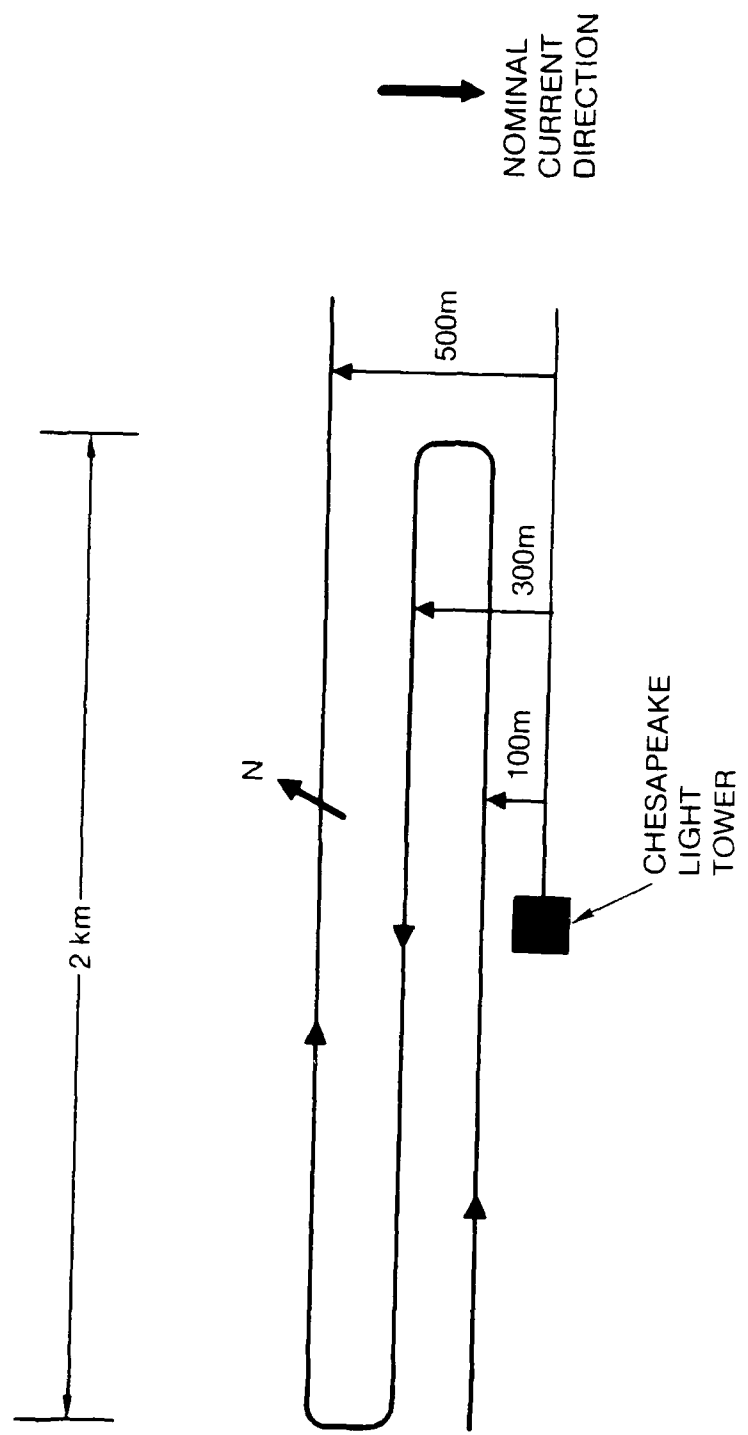


Figure 13. Schematic of a Typical Ship Pass.

VI. FIELD SITE INSTRUMENT MOUNTINGS

Pre-experiment site preparation is essential to the experiment. This includes close coordination of instrument placement and the evaluation of each instrument location on the tower to insure that proposed mounting specifications are possible, and that each assembly of instruments can function properly once installed.

The handling of heavy equipment (such as the wave follower, booms for instrument mounting, and two electric power generators) is accomplished with the use of a mobile crane. The crane weighs nearly 500 kg. It has a 7.5 ton lift capacity and a 6.1m hydraulic boom which can rotate 360 degrees. The boom is equipped with a 61m cable reel to maximize load reach. The crane is used for loading and off loading at the shore staging area. It is transported by helicopter and placed on the tower helicopter deck for general purpose use.

Sufficient power is provided to meet the experimental requirements of SAXON I investigations. A 40 kW generator is devoted to running the tower facility. Two additional 50 kW generators are provided to support the specific power requirements of the experiment. One 50 kW generator is designated to support the power needs of the wave follower. A second 50 kW generator provides power for the various instrument systems. Cabling is routed to the wave follower and to the other instrument systems, as required.

The following breakdown shows the placement of independent instrument systems at each level of the tower:

A. Independent Systems

1. Subsurface Level

a) Thermistor Array - Four 28 element thermistor arrays are suspended by strain members from the corners at each leg of the tower for the recording of internal wave activity. These are shown in Figure 14. In addition, a portable sparse array is to be fabricated to serve as an "early warning" internal wave monitor. It is deployed in the up-wave direction (or to the east) of the tower.

b) Pressure Sensors - Approximately 18 pressure sensors are placed at the -6m level positioned diagonally across the tower from leg to leg, as shown in Figure 14. Additional sensors are placed just below the sea level, either beneath the tower or (<30m) to

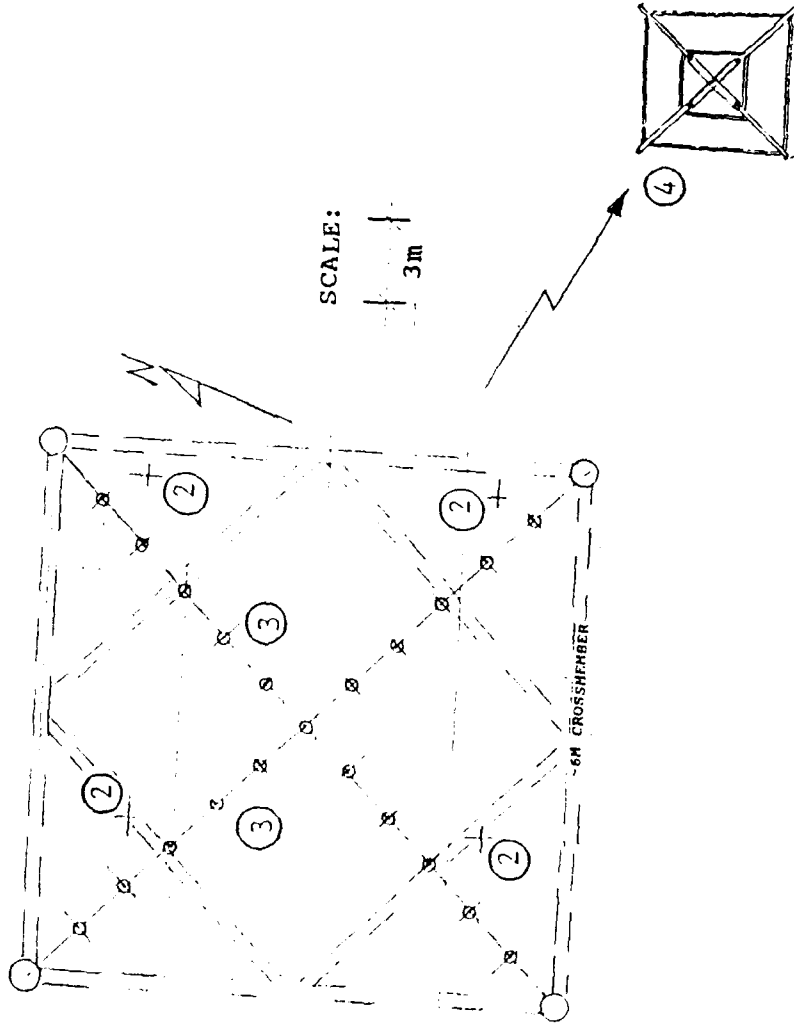


Figure 14. View of Underwater Instruments Mounted as Seen Looking Downward to the Base of Tower, -6m Level. 1. Wave Slope Sensor - (Not Shown), 2. Thermistor Arrays, 3. Pressure Sensors, 4. Doppler Current Meter Located approximately 50m South East of Tower Base.

the east to reduce contamination of the wave field by the tower structure. An additional square (2m x 2m) array of four pressure sensors is mounted 5m below the surface on the tripod located at a distance of 50m from the south east corner of the tower.

c) Current Meter - A coherent Doppler acoustic current meter is mounted on a tripod, as shown in Figure 15, positioned below the mean water level, and within 50m off the south-east corner of the tower.

2. Surface Level

In-situ measurements of surface films are obtained in support of the SAXON I experiment. During significant experimental events the following are obtained:

(i) In-situ single point determinations of sea surface tension at the base of the tower.

(ii) Collection of occasional water samples for later analysis at the Naval Research Laboratory, where the film pressure vs. area isotherms are determined and compared to similar data from the field sites investigated in the Marine Microlayer Program.

(iii) Continuous monitoring of the surface tension of water delivered from a floating pump to a sensor mounted on the tower. The apparatus design closely approximates that used for the same purpose in the TOWARD experiment.

3. Catwalk Level

a) Surface Tension Measurements - The CLT gantry crane extension, located at the north-west side of the tower, is used to hold the laser optics to deflect a laser beam down to the ocean surface. A wire cable is suspended from this location downward to the 5m catwalk level. The end of the cable is fastened to a mounting plate that mates to a plate attached to a telescope used to direct the laser beam to the ocean surface. The telescope is held in place by a 10m extension ladder which is braced against the tower at the 5m level, and a guy wire added for additional stability, as shown in Figure 16. The mobile crane is used to raise and lower the telescope for daily servicing.

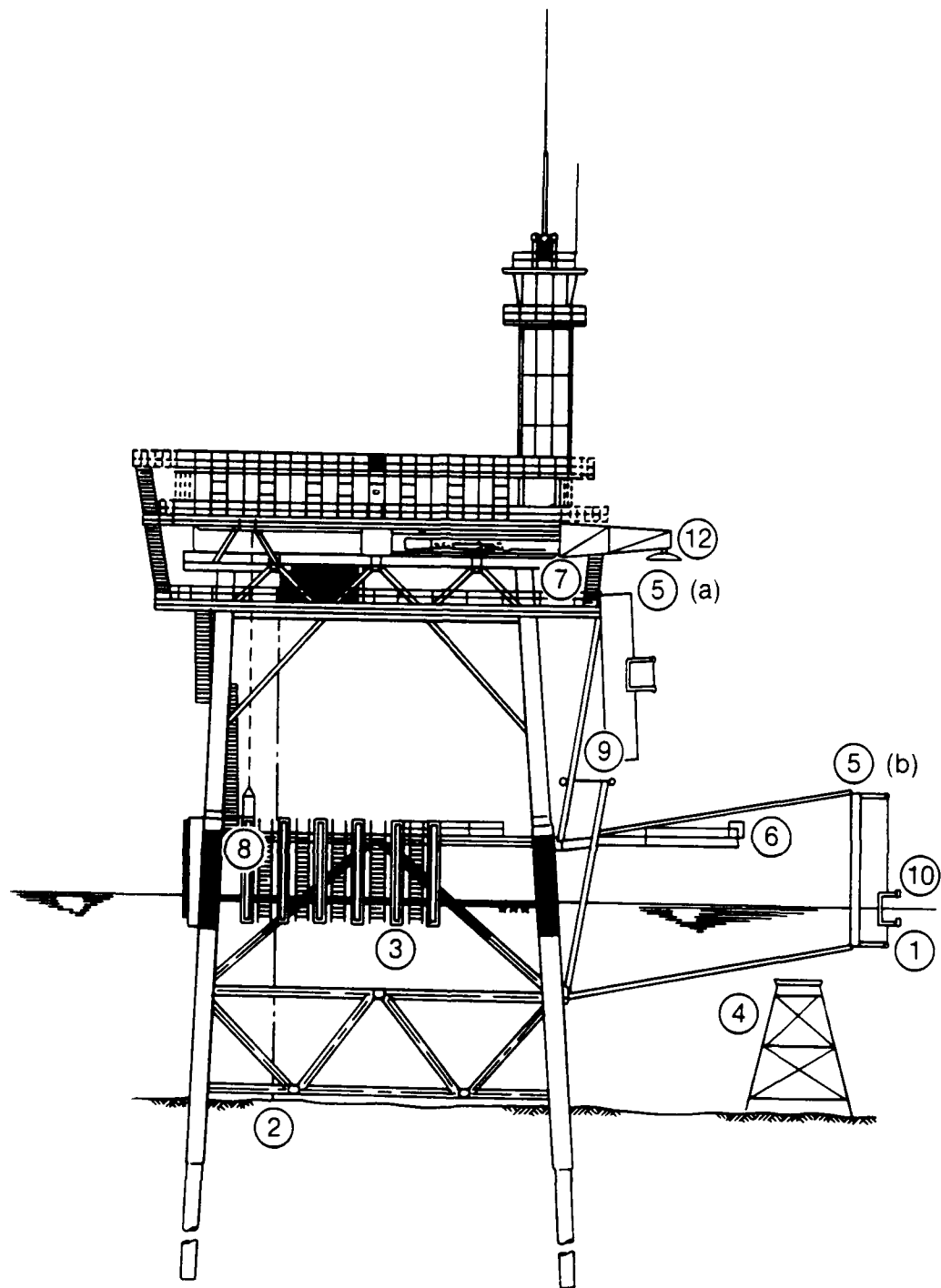


Figure 15. View of Instruments as Seen Looking from West Elevation. 1. Wave Slope Sensor, 2. Thermistor Arrays, 3. Pressure Sensors, 4. Doppler Current Meter. 5. (a) Wave Follower in Storage Position, (b) Wave Follower in Operating Position 6. Wind Drag and Short Wave Slopes, 7. Stillwell Photography, 8. Surface Tension, 9 Stereophotography T-Bar, 10. Surface Tension, 11. Not shown, 12. C- to W-Band Multi-Frequency Radar.

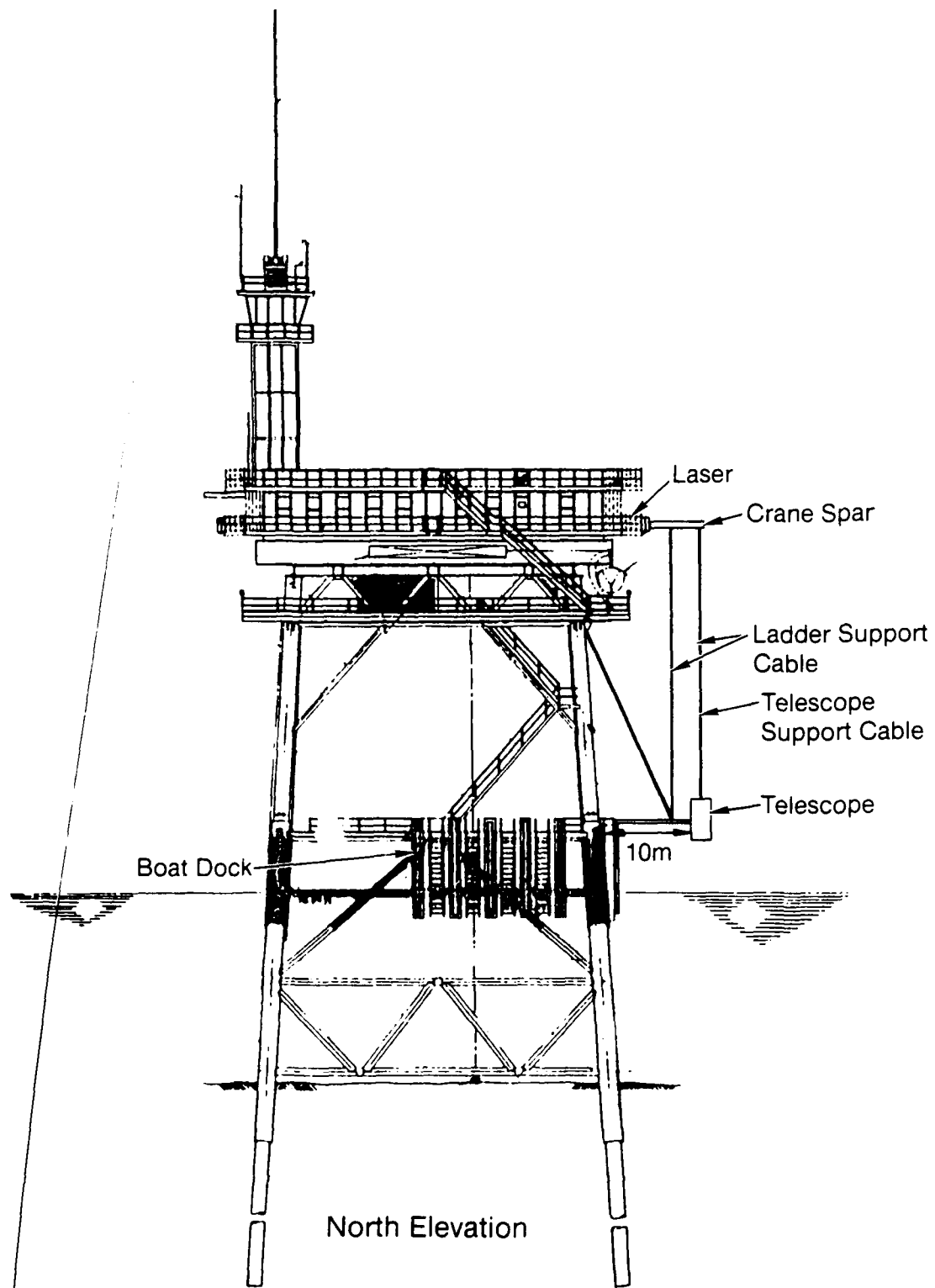


Figure 16. RPI Surface Tension Measurement System.

b) Stereophotography T-Bar - A T-Bar is mounted off the south-west corner of the tower structure, as shown in Figure 17. This is a 6.0m x 10m metal bar used for calibration of the stereo cameras which are mounted on the I-beam below the quarters deck level.

c) Wind Drag and Stability - A 19m boom is mounted off the south-east corner for instrument mounting, as shown in Figure 17. A catwalk along the boom provides for ease of instrument servicing.

d) Wave Measurements - A 6.6m boom is installed at the corner off the east face at the south-east (just north of the beacon tower), as shown in Figure 17. This boom is attached to the lowest catwalk and supports a wave gage array. The wave measurements are used in conjunction with the nadir-looking K_u band radar mounted directly above at the quarter deck level.

4. Main Deck Level

a) Stereophotography - Two synchronized cameras are deployed at this level, as shown in Figure 18. This is mounted in conjunction with the T-Bar located immediately below at the cat walk level.

b) Stillwell Photography Three cameras with break away brackets are mounted on the hand rail at this level, as shown in Figure 18. These are repositioned during the day from the south-east to the south-west corner, depending on the sun angle.

c) C-to W-Band Radar - This U-Ka radar is mounted on a 15.0m boom built of triangular cross-sections attached to a pillar and positioned to swing out from the tower between the main deck and the quarters deck levels at the south-west corner, shown in Figure 18. The vector slope gage and scatterometers are mounted on the same boom to facilitate comparison with the same point observed by the stereo-system.

5. Quarter Deck Level

a) Surface Tension Measurements - A 2.1m boom is installed at the north-west side of the tower off the hand rail. This is mounted in conjunction with a 6.1m boom located directly below at the cat walk level, as

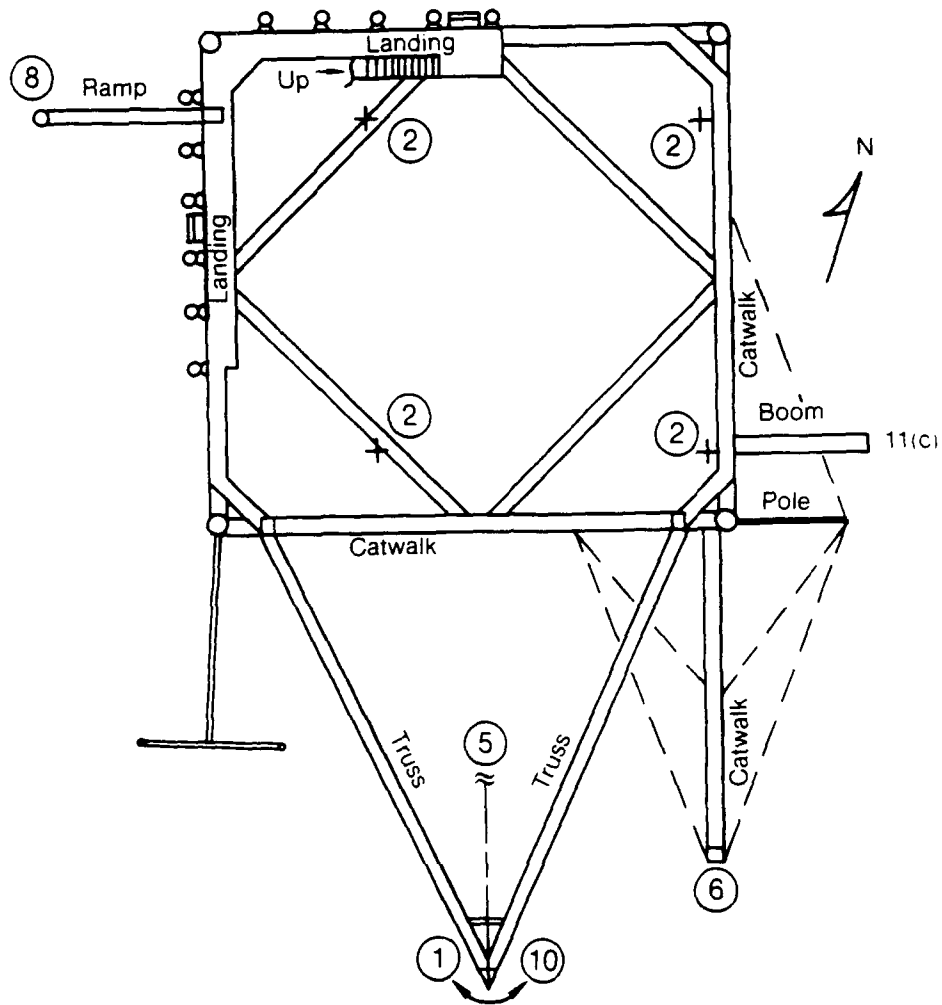


Figure 17. View of Instruments as Seen Looking Downward at Catwalk Level. 1. Wave Slope Sensor, 2. Thermistor Arrays, 3-4 (Not Shown), 5. Wave Follower, 6. Wind Drag and Short Wave Slopes, 7. (Not Shown), 8. Surface Tension, 9(b). Stereophotography T-Bar, 10, Surface Tension. 11(c). Wave Gage Array.

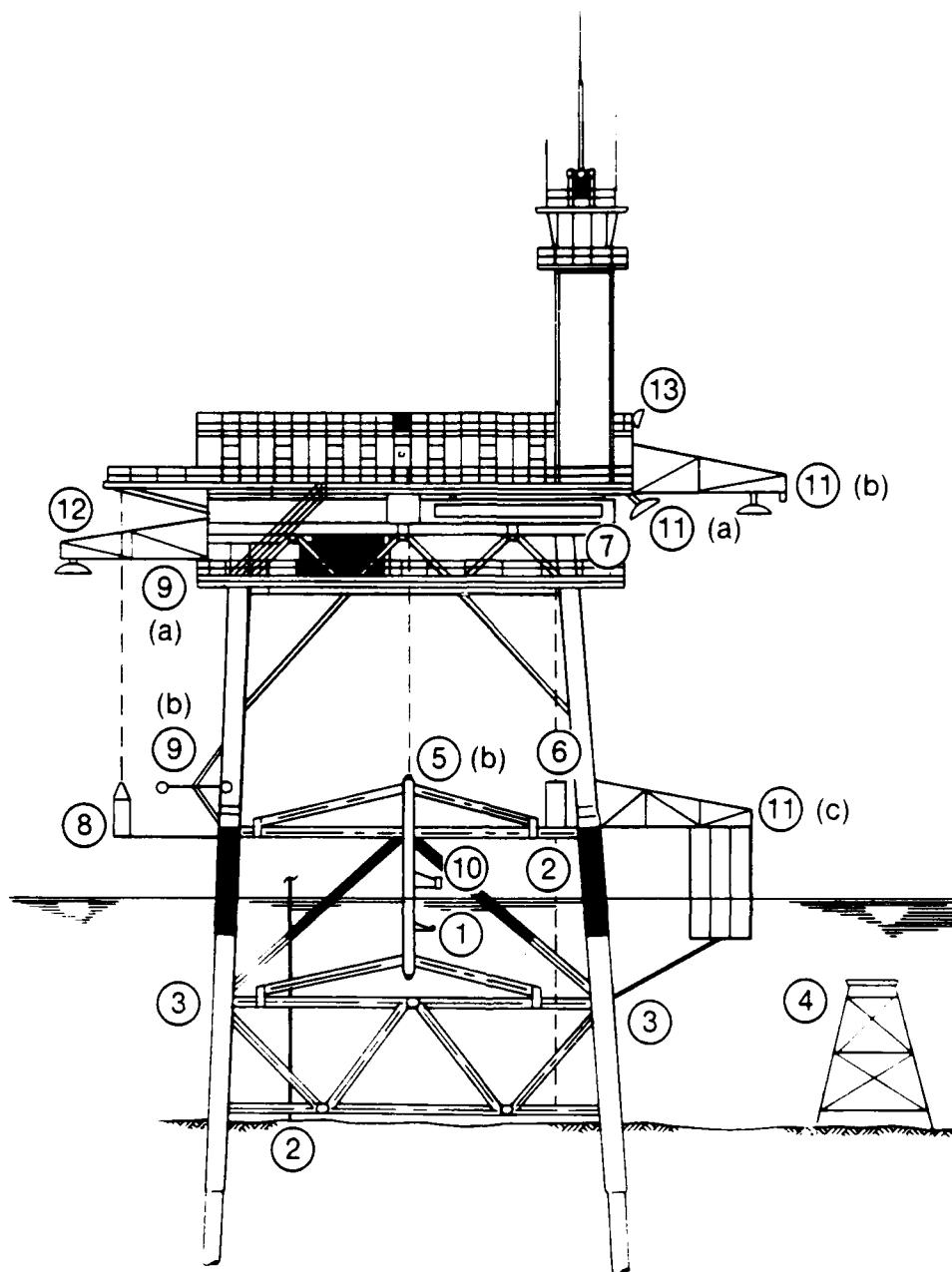


Figure 18. View of Instruments Mounted as Seen from South Elevation. 1. Wave Slope Sensor, 2. Thermistor Arrays, 3. Pressure Sensors, 4. Doppler Current Meter, 5 (a) (Not Shown), (b) Wave Follower in Operating Position, 6. Wind Drag and Short Wave Slopes, 7. Stillwell Photography, 8. Surface Tension, 9. (a) Stereophotography T-Bar, 9. (b) Stereophotography T-Bar, 10. Surface Tension, 11(a). K_u -Band Radar, 11(b). K_u -Band Radar and Wave Gauge, 11(c). Wave Gauge Array 12. C- to W-Band Multi-Frequency Radar, 13. C-, K_a - and G-Band Radar.

shown in Figure 18. Cables are routed into a service room at this location to support a co-axial power cable for the photomultiplier tube, and a standard co-axial cable for signal return. Similar cables run from this location to the 6.1m boom below.

b) Ku Band Radar and Thorn Wave Gage - This NRL nadir looking radar and wave gage are positioned on a 6.6m boom located 6m from the south-east corner extending off the east face, as shown in Figure 18. These measurements are used in conjunction with the wave gage measurements located at the catwalk level directly below.

c) Ku Band Radar - This NRL radar is mounted on the hand railing next to the K_u Band Radar and Thorn wave gage boom described in b) above, and as shown in Figure 18. This radar is set to operate with a 45 degree incidence angle.

6. Helicopter Level.

a) C-, K_a - and G-Band Radar - This University of Massachusetts radar is mounted on a 4.6m boom off the south-east corner of the tower, as shown in Figure 19.

b) NRL Radiometer System - This system is deployed on the rail at this level and operated with a 54 degree incidence angle.

B. Wave Follower

The present wave follower is deployed off the south side of the tower from the 5m cat walk level and the -6m horizontal structural level, as shown in Figure 18. The wave follower is fastened to the tower by an A-Frame parallelogram that extends to 17.7m from the tower. The 11.6m vertical trestle mounted to the A-Frame, provides for a continuous cable assembly allowing the C-Frame platform to move vertically, hence maintaining a constant submergence depth as it rides on the long waves. Upon completion of the experiment, the C-Frame will be dismantled and the wave follower stowed against the tower structure, as shown in Figure 15.

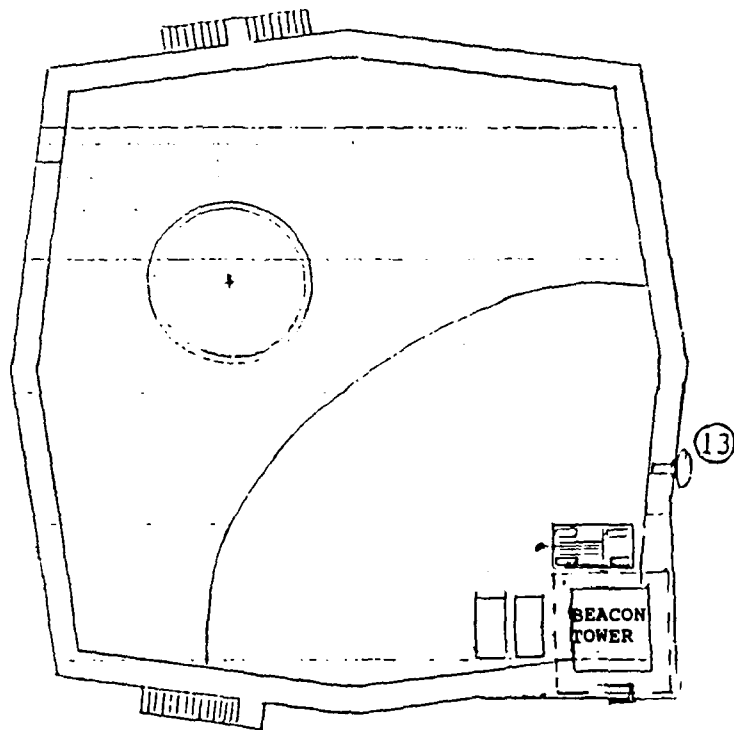


Figure 19. 13. C-, K_a and G-Band Radar Instruments Mounted as Seen Looking Down from the Helicopter Deck Level.

The instruments mounted on the C-Frame include:

1. Laser Optical Sensor - This instrument weighs 2.3 kg and is positioned so that the optical instrument is mounted on the upper face of the C-Frame, and the laser is mounted on the lower face of the C-Frame facing upward.

2. Surface Light Scattering Spectrometer - This instrument weighs 2.3 kg and is mounted on the C-Frame. The sensor beam is positioned side by side in relation to the laser-optical sensor beam location. The sensor is operated to measure surface tension simultaneously with surface slope measurements.

3. Acoustic Doppler Velocimeter - This instrument weighs 2.3 kg, is 6.4 cm in diameter and is 76 cm long. It is positioned along side the laser. The sensor tip is positioned approximately 7 cm below the surface.

4. Electromagnetic Current Meter - This current meter is mounted on the lower face of the C-Frame and provides the two horizontal components of the current immediately below the laser beam spot on the ocean surface.

C. Circular Wave Generator

The system, also known as "Bobbing Buoy", was operated in TOWARD to generate 30 cm long surface waves. In SAXON, an improved version is operated to generate circular waves in the range 3-30 cm. The system operates as a vertically oscillating buoy with a preset frequency. The buoy frequency is recorded at the tower. The decay rate of the circular waves will be measured using stereophotography.

VII. EXPERIMENT COORDINATION AND MEASUREMENT STRATEGY

For the field operations a coordination center is established at the U.S. Coast Guard Light House Station located on Cape Henry, Fort Story Army Post. This location serves as the staging area for on/off loading of all heavy equipment being transported to and from the Chesapeake Light Tower. Transportation to and from the tower is provided by the U.S. Coast Guard and a chartered vessel. The U.S. Coast Guard has two 12m and one 25m cutter (Figure 20) servicing the area. Departure is from the Little Creek Coast Guard Station. The 12m cutters can moor along side of the tower. The 25m requires that personnel on/off load at least 100m away from the tower via a rubber utility raft, as shown in Figure 21.

The scientific and logistical considerations are coordinated in accord with the organization plan, shown in Figure 22. The Principal Investigator in consultation with individual investigators reviews flight availability and readiness, surface instrument readiness, and environmental conditions to formulate decisions for use of aircraft and/or coordination of tower measurements. Daily weather and wave forecasts are obtained from the Navy Eastern Oceanographic Center at Norfolk (NEOC) and used to determine strategy of measurement during the following day.

The Test Director is responsible for implementation of the experiment plan in accord with the above decisions. The Test Director is the single point of contact for directives regarding the day-to-day operations of the experiment.

Experiment readiness reviews are held each day during the test period. Direct teleconference links are established with each of the staging element areas.

The SAXON I Project Schedule of Events is shown in Figure 23.

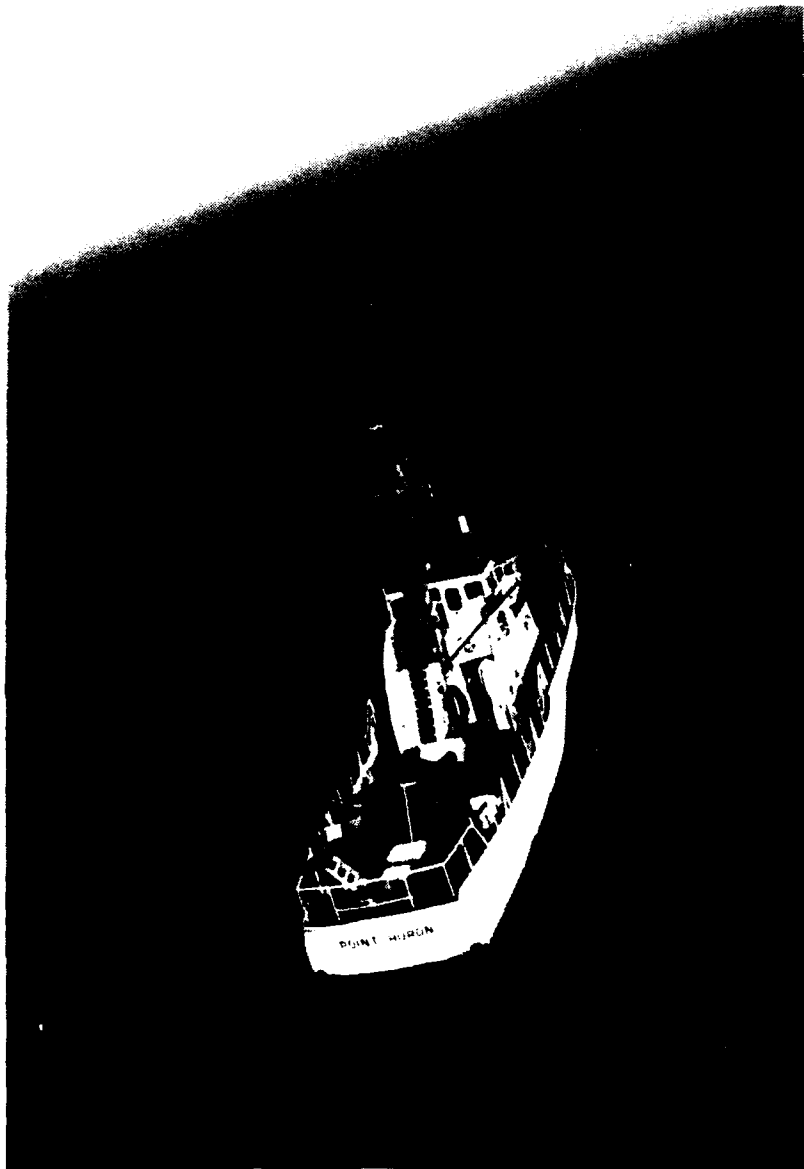


Figure 20. U.S. Coast Guard 25m Cutter Point Huron. One of Three Cutters will be made Available for Transportation to the Tower on a non-interference basis.



Figure 21. Rubber Raft Used by 25m Cutter to On/Off Load Personnel to and from the Chesapeake Light Tower. 12m Cutters Can On/Off Load directly at this Tower Landing.

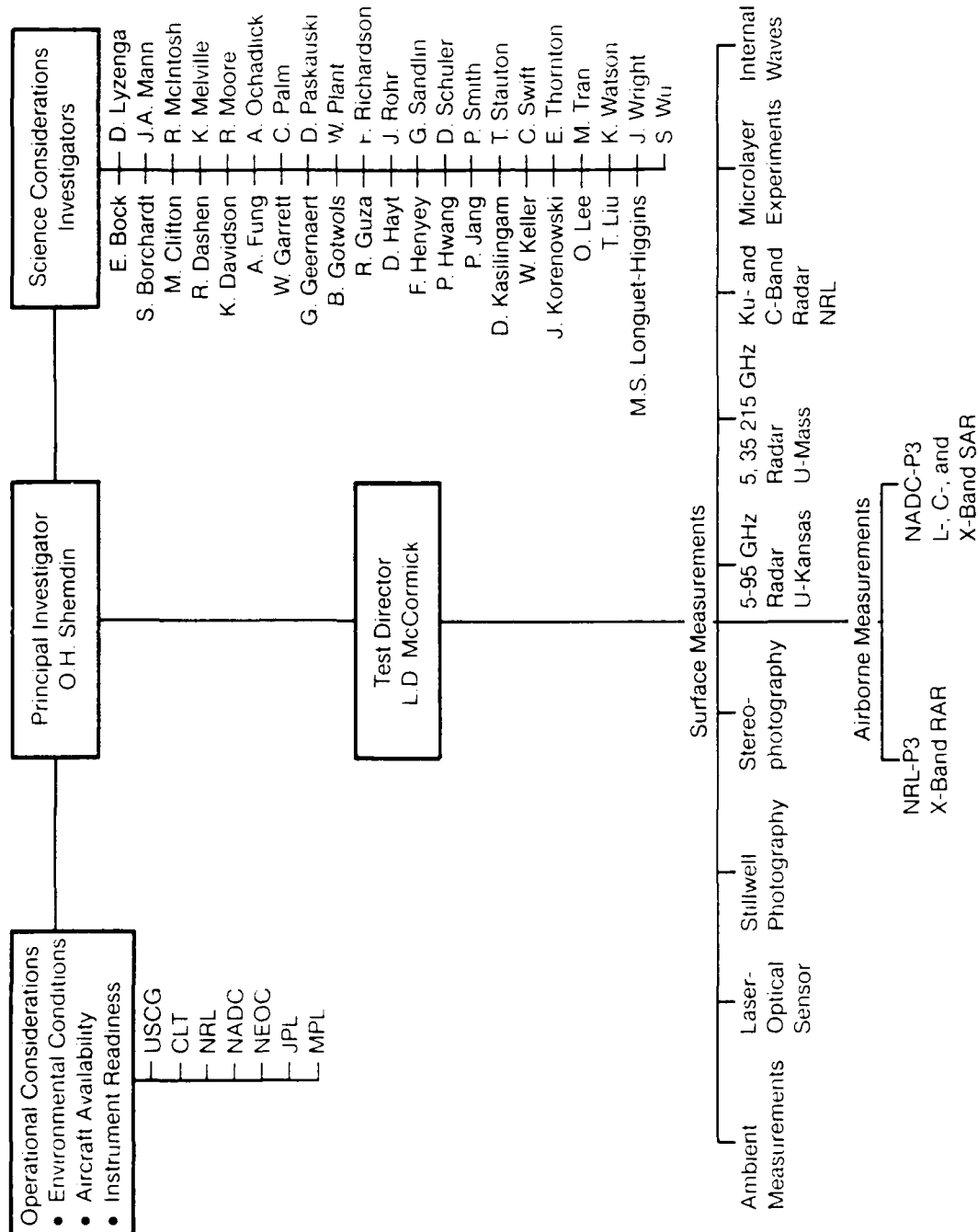


Figure 22. Organization Plan for SAXON I Experiment.

VIII. DATA MANAGEMENT

It is planned that a Data Management Center, Figure 24, be established for the purpose of collecting, organizing, safeguarding, and accounting for the distribution of the various data sets obtained from each participating organization.

Each investigator shall be responsible for providing the Data Center with the predetermined data logs and all information related to their activities that is required by other investigators.

The Data Center will provide each investigator with the daily environmental measurements. All aircraft images will be collected and maintained on file for distribution to investigators, as needed. Further, the Data Center is to maintain logs of all data sets collected for distribution to investigators. Data reports submitted to the Center by each investigator will be made available to all the other SAXON I participants without cost.

The Data Center will utilize a computer system that is adequate for meeting the above requirements. It is expected that the Data Center will be staffed with a qualified individual responsible for management of the Center in accordance with the overall objectives of the SAXON I Science Plan.

All data acquired in SAXON I will be made available at large, at the expense of the requester, in accordance with the Freedom of Information Act, one year after instruments are pulled out of the water. A data survey report will be prepared by 1 January 1989. Data reports are to be submitted by June 1989.

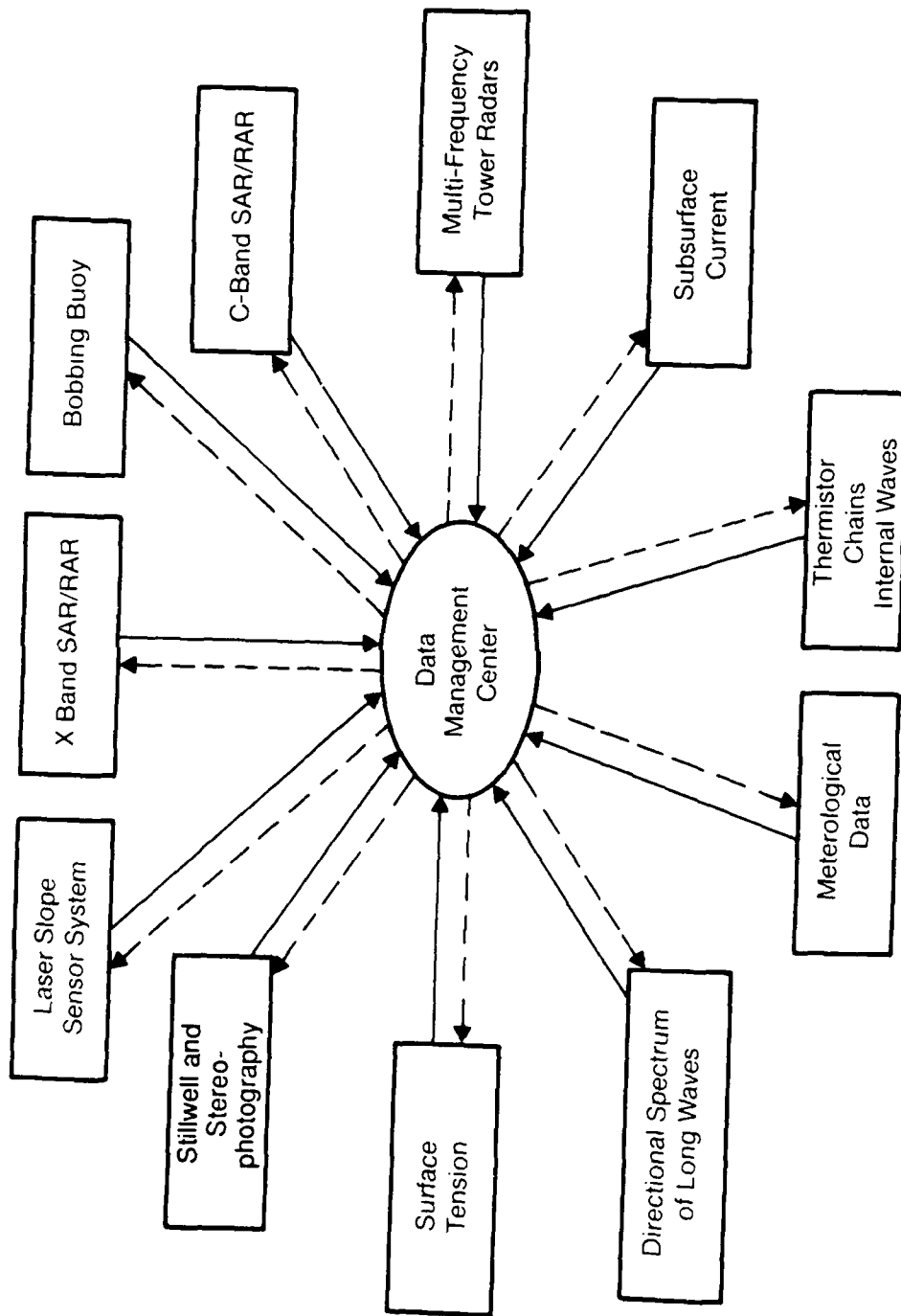


Figure 24. Data Management Center for SAXON I Experiment.

IX. DATA ANALYSIS

Two primary areas of analysis will be emphasized in the data analysis phase. These are:

1. Hydrodynamics of very short waves.
2. Radar backscatter modulations due to internal and long surface waves.

The above will require supporting analyses related to:

1. Subsurface hydrodynamics.
2. SAR imaging.

Tables 7a and 7b show the participating investigators and related areas of analysis.

Table 7a. Investigators and Corresponding Areas of Analysis.

Organization	Supporting Analysis		Radar Backscatter	Supporting Analysis
	Subsurface Hydro-dynamics	Surface Hydro-dynamics		SAR/RAR Imaging
APL/JHU		B. Gotwols R. Sterner R. Chapman		
DTI	P. Jang			
GSFC/NASA	T. Liu			
ISA	O. Lee			
JPL		R. Martin		T. Thompson W. Brown R. Goldstein H. Zebker F. Li
LJI		F. Henyey	J. Wright	M.S. Longuet-Higgins
MIT				J. Henry
MPL	P. Hanson	K. Watson P. Hanson		
NADC				A. Ochadlick
NORDA		P. Smith		

Table 7b. Investigators and Corresponding Areas of Analysis
(Continued).

Organization	Supporting Analysis		Supporting Analysis	
	Subsurface Hydro-dynamics	Surface Hydro-dynamics	Radar Backscatter	SAR/RAR Imaging
NOSC	J. Rohr			
NPGS		K. Davidson E. Thornton T. Stanton		
NRL		W. Barger G. Geernaert D. Schuler	W. Keller	W. Plant C. Sandlin/ J. Hollinger
ORE		P. Hwang M. Tran	D. Kaslingam	D. Hayt
ORINCON		W. Garrett		
RPI		J. Korenowski W. Asher		
SIC	S. Beck	R. Guza		
U TEXAS ARLINGTON			A. Fung	
U DELAWARE		J. Wu		D. Lyzenga
U KANSAS			R. Moore	
U MASS			C. Swift	
USGS		S. Wu		

REFERENCES

- Dynamic Technology, Inc. (1987) Perspectives on Future Research Directions in Ocean Remote Sensing, Report No. DTN-BP701-01, 23 pps.
- Geernaert, G.L., K.L. Davidson, S.E. Larsen and T. Mikkelsen (1987) Wind Stress Measurements During the Tower Ocean Wave and Radar Dependence Experiment, Accepted for Publication in JGR.
- Holiday, D.G. St-Cyr and N.E. Woods (1986) A Radar Ocean Imaging Model for Small to Moderate Incidence Angles, Int. J. Remote Sensing, 7, pp. 1809-1834.
- Hsiao, S.V. and O.H. Shemdin (1983) Measurement of Wind Velocity and Pressure with a Wave Follower, J. Geophys. Res., 88, 9841-9849.
- Hughes, B.A. (1978) The Effect of Internal Waves on Surface Wind Waves, 2. Theoretical Analysis, J. Geophys. Res., 83, 455-465.
- Hwang, P.A. and O.H. Shemdin (1988) The Dependence of Sea Surface Slope on Atmospheric Stability and Swell Conditions, Accepted for Publication in JGR.
- Jang, P.S. (1986) Comparison of Composite Two-Scale Radar Scattering Model with Full Wave Approach, Dynamic Technology, Inc. Report DT-8607-10.
- Kasilingam, D.P. and O.H. Shemdin (1988) A Comprehensive Theory for Synthetic Aperture Radar Imaging of the Ocean Surface: With Application to TOWARD on Focus, Resolution and Wave Height Spectra, Accepted for Publication in JGR.
- Lubard, S. C., R. W. Ziemer and J. B. Swan (1974) OWEX/FLIP Radar Experiment Summary Report (U), RDA Report No. RDA-SR-010-ARPA, 71 pps.
- Paskausky, D., J.D Elms, R.G. Baldwin, P.L Franks, C.N. Williams, Jr., and K.G Zimmerman (1984) Addendum to Wind and Wave Summaries for Selected U.S. Coast Guard Operating Areas. National Climatic Data Center Asheville, NC 28801, Report No. CC-D-05-84, 523 pps.
- Pierson, W.J., Jr. and R.A. Stacy (1973) The Elevation, Slope and Curvature Spectra of Wind Roughened Sea Surface. NASA Tech Report No. CR - 2247, 126 pps.
- SARSEX Interim Report by the SARSEX Experiment Team, JHU/APL STD-R-1200, May 1985.

Shemdin, O.H. (1966) The Dynamics of Wind in the Vicinity of Progressive Water Waves, Ph.D. Dissertation, Stanford Univ., Stanford, California.

Shemdin, O.H. (1980) Measurement of Wind and Surface Wave Slopes with a Wave Follower, JPL Report No. 715-123, Pasadena, California.

Shemdin, O.H. and P.A. Hwang (1988) Comparison of Measured and Predicted Sea Surface Spectrum of Short Waves, Accepted for Publication in JGR.

Shemdin, O.H., S. Wu and M. Tran (1988) Stereo Photographic Observations of the Sea Surface in TOWARD, Accepted for Publication in JGR.

Synthetic Aperture Radar Working Group Interim Report, Volume I (S), 1986.

TOWARD Experiment Team (1986) TOWARD Field Experiment Interim Report: Volumes I and II, JPL Report, Pasadena.

Valenzuela, G.R. (1978) Theories for the Interaction of Electromagnetic and Ocean Waves: A Review, Boundary Layer Meteorology, 13, 63-85.

Watson, K. (1986) Some Surface Wave Modulation Mechanisms Relating to the JOWIP and SARSEX Observation, Mitre Corp. JSR-85-203.

LIST OF TABLES

TABLE	PAGE
A-1 Other Aircraft and Respective Frequencies	69
A-2 System Characteristics of CCRS C- and X-Band SAR System On Board CV-580 Aircraft	70
A-3 CCRS Data Processing Characteristics	71
A-4 System Characteristics of MIT K_a -Band SAR/RAR System On Board Gulfstream Aircraft	73
A-5 Gulfstream SAR Data Processing Characteristics	74
A-6 System Characteristics of JPL P-, L- and C-Band SAR System On Board DC-8 Aircraft	75
A-7 JPL-SAR Data Processing Characteristics	76
A-8 System Characteristics of DFVLR X- and K_a -Band RAR System On Board Do228 Aircraft	77
A-9 System Characteristics of Intera X-Band SAR System On Board Conquest Aircraft	79
A-10 Intera STAR I System Data Processing Characteristics ...	80

APPENDIX A

DATA ON OTHER AIRCRAFT

I. Introduction

The inclusion of the airborne radar systems described below would have greatly enhanced the overall objectives of SAXON I. The consequence would have been a more comprehensive intercomparison of SAR and RAR imaging at a broader range of radar frequencies.

II. Desired Airborne Measurement Systems

The desired radar systems are shown in Table A-1. The radar characteristics for these are discussed below:

1. CCRS: C- and X-Band SAR on Board CV-580

A new generation Synthetic Aperture Radar (SAR) has been installed into the CCRS aircraft. It is a digitally controlled, two-channel radar, operating at C-Band (5.3 GHz), transmitting either H or V polarizations, and receiving both simultaneously. A breakdown of the specifications are shown in Table A-2. The system features an on board 7-look, real-time processor and display for one receive channel with data acquisition geometry in three modes; nadir, narrow swath, and wide swath. The system data processing characteristics are shown in Table A-3. During flight, data is sent to a dry silver image recorder and to HDDT. Measurements for this output show that the aspect ratio, averaged from 25 km section imagery, is correct to within 0.5%.

A dual-channel, X-Band system has recently been completed for installation into the aircraft.

Table A-1. Other Aircraft and Respective Frequencies.

Aircraft	SAR Mode					RAR Mode		
	P	L	C	X	K _a	C	X	K _a
1. CCRS CV-580			.	.				
2. MIT Gulfstream					.			.
3. NASA DC-8	.	.	.					
4. DFVLR Do228			.	¹			.	.
5. INTERA CONQUEST				.				

¹Available in 1989

Table A-2. System Characteristics of CCRS C- and X-Band SAR System
On Board CV-580 Aircraft.

	<u>C-Band</u>
Center Frequency (GHz)	5.3
Wavelength (cm)	5.6
Pulse Length (Msec)	7
Bandwidth (MHz)	37
Peak Power (kW)	27
Antenna Azimuth Beam Width (deg)	H-3.6 / V-4.2
Antenna Range Beam Width (deg)	23
Antenna Beam Center Gain (dB)	24
Nominal Altitude (km)	6
Nominal Ground Speed (m/s)	131
Flight Duration (hrs)	6
Nominal PRF (pps/pol) at 257 m/s	350 Hz
Swath Width - Quad Pol Mode (km)	22
Resolution (7 Looks)	10 x 6
Slant Range(m) x Azimuth(m)-Digital	0-74°
Incident Angle	HH, VV, HV, VH
Polarization	30 dB Digital,
Linear Dynamic Range - Power	

Table A-3. CCRS Data Processing Characteristics.

Polarizations	HH - VV - HV - VH
Angle of Incidence at Center of Image	35°
Digital Slant Range Coverage	22 km
Digital Along Track Coverage (Raw)	16 km
Digital Along Track Coverage (Image)	16 km
Digit Image Size	4096 pixels range x 4096 pixels azimuth
PRF	2.57 x (Ground Speed in m/s) 337 @ 131 m/s
Digital Image Pixel Spacings	4.0m Slant Range x 3.89 azimuth

2. MIT K_a-Band System on Board Gulfstream Aircraft

This system is in its final stages of development and is expected to be in operation by Summer 1988. The system characteristics are shown in Table A-4; it can be operated in both SAR and RAR modes, simultaneously. The data processing characteristics are shown in Table A-5.

3. JPL P-, L- and C-Band Radar on Board NASA: DC-8 Aircraft

The JPL L-Band system on board the NASA: CV-990 was flown in TOWARD with a high degree of success because of the simultaneous digital and optical recordings and image processing capabilities available with the system. The system is expanded to include C- and P-Bands with multi-polarizations and is deployed on the NASA: DC-8. Table A-6 shows the system characteristics. The data can be obtained with various imaging geometries such as aircraft altitude and azimuthal angles relative to surface waves and/or wind direction. The data processing system characteristics are shown in Table A-7. The versatile polarimetric capabilities of this radar system will allow determination of the coherence time of surface scatterers. This important information will be compared with other determinations of the same quantity using tower-based radars.

Both the L- and C-Band radars have front and back antennas. The system is operated as an interferometric SAR where phase difference measurements are obtained on a pixel-by-pixel basis. These are converted to line-of-sight velocities for use in verifying velocity bunching and other velocity-related aspects in SAR imaging.

4. DFVLR X- and K_a-Band RAR on Board Do228

It would have been desirable to have the participation of the German Aerospace Research and Development Institution. Their X- and K_a-Band RAR system would be deployed on a Do228 aircraft capable of making a flight across the Atlantic Ocean. The RAR has been operated for detection of sea slicks and has produced good quality images. The specifications of this system are detailed in Table A-8. A C-Band SAR will be available in 1989. The corresponding resolution will be better than 10.0m.

Table A-4. System Characteristics of MIT/K_a-Band SAR/RAR System
On Board Gulfstream Aircraft.

Center Frequency (GHz)	33.56
Wave Length (cm)	0.89
Pulse Length (μsec)	30
Bandwidth (MHz)	600
Peak Power (kW)	84
Azimuth Beam Width (deg)	2.1
Antenna Range Beam Width (deg)	40
Incidence Angle (deg)	40-80
Nominal Altitude (km)	5.0
Nominal Ground Speed (m/s)	103
Flight Duration (hrs)	5
Nominal PRF (pps/pol) at 257 m/s	1,500
Swath Width - Quad Pol Mode (km)	0.7
Resolution	
Slant Range (m) x Azimuth (m) - Digital	3.0 x 3.0
Polarization	HH, VV, HV, VH
Absolute Cross Section Accuracy (dB)	±2.0
Relative Cross Section Accuracy (dB)	±0.5
Clutter to Noise Ratio (dB)	20
Pixel Registration (m)	1
Aircraft Position Accuracy (m)	±15

Table A-5. Gulfstream SAR Data Processing Characteristics.

Polarization	HH, VV, HV, VH
Angle of Incidence at Center of Image (can be adjusted)	60
Digital Slant Range Coverage	0.7 km
Digital Along Track Coverage (Raw)	30 km
Digital Along Track Coverage (Image)	30 km
Digital Image Size	—
Optical Image Size	—
PRF (pps)	1500
Digital Image Pixel Spacings	—

Table A-6. System Characteristics of JPL P-, L-, and C-Band SAR System
On Board DC-8 Aircraft.

	<u>P-Band</u>	<u>L-Band</u>	<u>C-Band</u>
Center Frequency (GHz)	0.44	1.25	5.3
Wavelength (cm)	68	24	5.7
Pulse Length (μ sec)	10	10	10
Bandwidth (MHz)	20	20 \rightarrow 40	20 \rightarrow 40
Peak Power (kW)	1.0	5.0	1.0
Antenna Azimuth Beam Width (deg)	21.4	8.6	2.3
Antenna Range Beam Width (deg)	75	75	75
Antenna Beam Center Gain (dB)	12	17	24
Nominal Altitude (km)	6-12	6-12	6-12
Nominal Ground Speed (m/s)	216	216	216
Flight Duration (hrs)	12-16	12-16	12-16
Nominal PRF (pps/pol) at 257 m/s	600	600	600
Swath Width - Quad Pol Mode (km)	17	17	17
Resolution (4 Looks)			
Slant Range(m) x Azimuth(m)-Digital	7.5 x 8.0	7.5 x 8.0	7.5 x 8.0
Incident Angle	0-75 deg	0-75 deg	0-75 deg
Polarization	HH, VV, HV, VH	HH, VV, HV, VH	HH, VV, HV, VH
Linear Dynamic Range - Power	_____	22 dB Digital, 12 dB Optical	_____

Table A-7. JPL-SAR Data Processing Characteristics.

Four OPTICAL Channels	HH - VV - HV - VH
4 DIGITAL SUBFRAMES	HH - VV - HV - VH
Angle of Incidence at Center of Image	35°
Optical/Digital Slant Range Coverage	7 km (Quad Pol Mode)
Optical/Digital Slant Range Coverage	12 km (Quad Pol Mode)
Optical Along Track Coverage	60 km
Digital Along Track Coverage (Raw)	30 km
Digital Along Track Coverage (Image)	11 km
Digital Image Size	927 pixels range x 1024 pixels azimuth
Optical Image Size	50 mm cross track, 1:250,000 along track
PRF	3 x (CV-990 Ground Speed in m/s) 600 @ 200 m/s, 750 @ 250 m/s
Digital Image Pixel Spacings	7.5m Slant Range x 11.0 Azimuth

Table A-8. System Characteristics of DFVLR X- and Ka-Band RAR System
On Board B. 228 Aircraft.

	X-Band	Ka-Band
Center Frequency (GHz)	9.3	35
Wavelength (cm)	3.0	0.89
Pulse Length (Msec)	60	---
Bandwidth (MHz)	---	---
Peak Power (kW)	23	20
Antenna Azimuth Beam Width (deg)	0.5	0.5
Antenna Range Beam Width (deg)	45	20
Antenna Beam Center Gain (dB)	---	---
Nominal Altitude (km)	1-3	1-3
Nominal Ground Speed (m/s)	77	77
Flight Duration (hrs)	---	---
Nominal PRF (pps/pol) at 257 m/s	---	---
Swath Width - Quad Pol Mode (km)	---	---
Resolution		
Slant Range (m) x Azimuth (m) - Digital	10 x 21	---
Incident Angle	68	68
Polarization	VV	---
Linear Dynamic Range - Power	70 dB	---

A new instrument, Rotating Synthetic Aperture Radar (ROSAR), which allows SAR imaging from a stationary platform, has been developed. This system provides a SAR image at 360 degrees around its position. It operates at L-Band, 1.15 GHz and can be operated from a tower together with a rotating RAR.

5. Intera X-Band On Board Conquest

The Intera STAR I, X-Band SAR system on board Conquest is a new generation SAR providing wide or narrow swath coverage with digital processing. The system characteristics are shown in Table A-9. Data recorded on the aircraft may be down-linked as imagery to a designated facility in real-time mode or produced as hard copy. SAR imagery is recorded on HDDTs and displayed on a continuous strip image recorder. Imagery produced on HDDTs can be transcribed to industry standard 6250 or 1600 bpi tapes. This production system is shown in Table A-10.

Table A-9. System Characteristics of Intera X-Band SAR System
On Board Conquest Aircraft.

	<u>X-Band</u>
Center Frequency (GHz)	10.0
Wavelength (cm)	3
Pulse Length (μ sec)	---
Bandwidth (MHz)	---
Peak Power (kW)	8
Antenna Azimuth Beam Width (deg)	---
Antenna Range Beam Width (deg)	---
Antenna Beam Center Gain (dB)	40 dB
Nominal Altitude (km)	9.5
Nominal Ground Speed (m/s)	144
Flight Duration (hrs)	4-6
Nominal PRF (pps/pol) at 257 m/s	---
Swath Width - Quad Pol Mode (km)	23
Resolution (4 Looks)	
Slant Range (m) x Azimuth (m)-Digital	6 in Range, 4 Azimth
Incident Angle	45°-70°
Polarization	HH
Linear Dynamic Range - Power	45 digital, 0 optical

Table A-10. Intra STAR I System Data Processing Characteristics.

OPTICAL Channels	0
1 DIGITAL SUBFRAMES	HH
Angle of Incidence at Center of Image	55°
Digital Slant Range Coverage	23 km
Digital Along Track Coverage (Raw)	46 km
Digital Along Track Coverage (Image)	25 km
Digital Image Size	4096 pixels range x 96 pixels azimuth
Optical Image Size	—
PRF	—
Digital Image Pixel Spacings	12.0m Slant Range x 12.0 Azimuth

APPENDIX B

SAXON I
DIRECTORY

Mr. Bill Asher
Rensselaer Polytechnic Institute
Department of Chemistry
Troy, New York 12180-3590
(518) 276-8982

Dr. William Barger
Naval Research Laboratory
Chemical Division
6175
Washington D. C. 20375
202-767-3573

Mr. Steve Beck
Scripps Institute of Oceanography
Marine Physical Laboratory
San Diego CA 92152
(619) 534-1797
OMNET - MPL.SIO

Dr. Erik Bock
Rensselaer Polytechnic Institute
Department of Chemistry
110 8th Street
Troy, New York 12180-3590
(518) 276-8457

Dr. Steven R. Borchardt
Dynamics Technology, Inc.
Suite 801
1815 N. Lynn Street
Arlington, VA 22209
(703) 841-0990
OMNET - S.BORCHARDT

Dr. Gary Brown
Virginia Polytechnic Institute
and State University
Department of Electrical Engineering
Blacksburg, VA 24061

Dr. Walter E. Brown, Jr.
Jet Propulsion Laboratory
Mail Stop 183-701
4800 Oak Grove Drive
Pasadena, CA 91109
(818) 354-4321 4-2110 or 2658

Mr. Mike Clifton
University of California
San Diego
Scripps Institution of
Oceanography
La Jolla, California 92093
(619) 534-0593

Mr. Frank Dareff
Naval Air Development Center
Code 3024
Warminster, PA 18974

Dr. Roger F. Dashen
University of California,
San Diego
Physics Department
La Jolla, California 92093
(619) 534-6659/2230

Professor Kenneth Davidson
Naval Postgraduate School
Code 63-DS
Monterey, CA 93943
(408) 646-2309
OMNET - K.DAVIDSON

Mr. Hans Dolezalek
Office of the Chief of Naval Research
Code 112D1HD
800 N. Quincy Street
Arlington Virginia 22217-5000
(202) 696-4025 OR 4125
OMNET - H.DOLEZALEK

Dr. Adrian K. Fung
University of Texas
at Arlington
E. E. Dept. Box 19016
Arlington, TX 76019
(817) 273-3422

Dr. William D. Garrett
Orincon
Suite 904
1755 Jefferson Davis Hwy.
Arlington Va. 22202
(703) 892-9222 NRL202 767-1602/3185

Dr. Gary Geernaert
Naval Research Laboratory
Code 7784
Washington, D.C. 20375
(202) 767-1602 or 2095
OMNET - G.GEERNAERT

Professor P. Gogineni
University of Kansas Center
for Research, Inc.
2291 Irving Hill Dr. Campus West
Lawrence, KS 66045-2969
(913) 864-7734 OR 844-4615
OMNET - KANSAS.U.RSL

Dr. Richard Goldstein
Jet Propulsion Laboratory
4800 Oak Grove Drive
Pasadena, CA 91109
(818) 354-4321 4-6999 4-2647

Dr. Bruce Gotwols
Johns Hopkins University
Applied Physics Laboratory
Johns Hopkins Road
Laurel, MD 20810
(301) 953-5000 EXT: 4543
OMNET - B.GOTWOLS

Dr. Robert T. Guza
University of California
San Diego
Scripps Institution of Oceanography
La Jolla, CA 92093
(619) 534-0585

Mr. Paul A. Hanson
SAXON Systems Engineer
University of California, San Diego
Marine Physical Laboratory
P. Jordan
San Diego, California 92152
(619) 534-1795
OMNET - MPL.SIO

Dr. Eric O. Hartwig
Director, Environmental Sciences
Office of Chief of Naval
Research
Code 112
Arlington, VA 22217-5000
(202) 696-4590
OMNET - E.HARTWIG

Mr. David Hayt
Ocean Research & Engineering
255 South Marengo Avenue
Pasadena, CA 91101
(818) 568-1800

Dr. John C. Henry
Assistant Group Leader
Massachusetts Institute of
Technology Lincoln Laboratory
Battlefield Surveillance
P. O. Box 73
Lexington, Mass. 02173-0073
(617) 863-5500

Dr. Frank Henyey
Associate Director
Center for Studies of Nonlinear
Dynamics
La Jolla Institute
10280 N. Torrey Pines Road, #260
La Jolla, CA 92037
(619) 587-6020
OMNET - F.HENYEV

Mr. Tom Herbers
Scripps Institute of
Oceanography
San Diego CA 92152
(619) 534-0226

Dr. Frank L. Herr
Office of Chief of Naval Research
Oceanic Chemistry Program
Code 1122C
Arlington, VA 22217-5000
(202) 696-4591
OMNET - F.HERR

Cdr. William Hicklin
Naval Air Development Center
Warminster, PA 18974-5000

Mr. Don Hoff
Jet Propulsion Laboratory
Mail Stop 125-177
4800 Oak Grove Drive
Pasadena CA 91109
(818) 354-3138

Dr. Paul A. Hwang
Ocean Research & Engineering
255 South Marengo Avenue
Pasadena, California 91101
(818) 568-1800
OMNET - O.SHEMDIN

CWO J. J. Jensen
Commander
U.S. Coast Guard Group
Hampton Roads
4000 Coast Guard Boulevard
Portsmouth, Va. 23703-2199
(804) 483-8516

Mr. Andrew Jessup
Massachusetts Institute of Technology
Department of Civil Engineering
Room 48-20
Cambridge, Massachusetts 02139
(617) 253-6577

Dr. Dayalan P. Kasilingam
Ocean Research and Engineering
255 South Marengo Avenue
Pasadena, California 91101
(818) 568-1800
OMNET - O.SHEMDIN

Dr. W. C. Keller
Naval Research Laboratory
Code 7784
Washington, D.C. 20375
(202) 767-2095
OMNET - W.PLANT

Dr. Gerald Korenowski
Rensselaer Polytechnic Institute
Department of Chemistry
Troy, New York 12180-8982
(518) 276-8480 or 8982

Professor Haralambos N. Kritikos
Moore School of Electrical Eng.
University of Pennsylvania
Philadelphia, PA 19104
(215) 898 8112

Professor Jay K. Lee
Dept. of Electrical and Computer Eng.
Syracuse University, Link Hall
Syracuse, NY 13244-1240
(315) 423-4395

Mr. Owen S. Lee
Integrated Systems Analysts, Inc.
Marina Gateway
740 Bay Boulevard
Chula Vista CA 92010
(619) 422-7100

Dr. Fuk K. Li
Jet Propulsion Laboratory
Mail Stop T-1206-D
4800 Oak Grove Drive
Pasadena California 91109
(818) 354-2849

Professor M. S. Longuet-Higgins
The La Jolla Institute
10280 N Torrey Pines Rd.
La Jolla, CA 92037
42879-4141 or (818) 568-1802
OMNET - O.SHEMDIN

Professor J. Adin Mann, Jr.
Professor of Chemical Engineering
Case Western Reserve University
Department of Chemical Engineering
Cleveland, Ohio 44106
(216) 368-4150

Mr. Robert E. Martin
Manager
Jet Propulsion Laboratory
Instrumentation Section
Mail Stop 125-177
4800 Oak Grove Drive
Pasadena CA 91109
(818) 354-3145

Mr. Les Mc Cormick
Ocean Research and Engineering
255 South Marengo Avenue
Pasadena, California 91101
(818) 568-1800
OMNET - L.MCCORMICK

Professor Robert E. Mc Intosh
Professor
University of Massachusetts
at Amherst
Microwave Remote Sensing Laboratory
Electrical and Computer Engineering
Amherst, Mass 01003
(413) 545-0709
OMNET - C.SWIFT

Professor Ken Melville
Massachusetts Institute of Technology
Department of Civil Engineering
Room 48-331
Cambridge, Massachusetts 02139
(617) 253-6577
OMNET - W.MELVILLE

Dr. Richard Moore
University of Kansas
Center for Research, Inc.
Campus West
2291 Irving Hill Drive
Lawrence Kansas 66045-2969
(913) 864-4836
OMNET - KANSAS.U.RSL

CDR Thomas S. Nelson, USN
Deputy Director
Office of Naval Research
OCNR Code 112 D
800 Quincy Street
Arlington VA 22217
(202) 696-4395
OMNET - T.NELSON

Dr. Andrew Ochadlick
Naval Air Development Center
Code 3024
Warminster, PA 18974
(215) 441-1993

Mr. Bill O'Reilly
Scripps Institute of
Oceanography
La Jolla CA 92093
(619) 534-0226

Mr. Paul Pallo
Supervisor,
U.S. Coast Guard
Shore Maintenance Detachment
1240 E. 9th Street
Cleveland, Ohio 44199-2060
(216) 522-7601

Dr. Charles S. Palm
Charles Palm & Associates
2036 San Pasqual Avenue
Pasadena CA 91107
(818) 578-1472
OMNET - O.SHEMDIN

Dr. David Paskausky
United States Coast Guard
Research and Development Center
Oceanography Branch
U.S. Coast Guard R & D Center
Groton CONN 06340
(203) 441-2740

Dr. William J. Plant
Naval Research Laboratory
Code 7784
Washington, D.C. 20375
(292) 767-2095
OMNET - W.PLANT

Mr. Ivan P. Popstefanija
Student
University of Massachusetts
at Amherst
Microwave Remote Sensing Laboratory
Electrical and Computer Engineering
Amherst Massachusetts 01003
(413) 545-4675

Mr. Pete Richardson
Naval Research Laboratory
Code 7784
Washington, D.C. 20375
(202) 767-2095

Dr. Jim Rohr
Naval Ocean Systems Center
Code 634
San Diego, California 92152-5000
(619)-553-1604

Mr. Jack Sanders
c/o Professor J. Adin Mann, Jr.
Professor of Chemical Engineering
Department of Chemical Engineering
Case Western Reserve University
Cleveland, Ohio OH 44106
(216) 368-4150

Dr. Glen Sandlin
Naval Research Laboratory
Code 8311
Washington, D.C. 20375-5000

Dr. Omar H. Shemdin
Ocean Research and Engineering
255 South Marengo Avenue
Pasadena, California 91101
(818) 568-1800
OMNET - O.SHEMDIN

Mr. Chuck Skupniewicz
Naval Post Graduate School
Dept. of Oceanography
Monterey CA 93943
(408) 646-2563

Dr. Peter M. Smith
Naval Ocean Research and
Development Activity
Code 321
Stennis Space Center
NSTL, MS 39529/5000
(601)688-5267

Mr. Tim Stanton
Naval Post Graduate School
Department of Oceanography
Monterey, California 93943
(408) 646-3144

Mr. Bob Steinbacher
Jet Propulsion Laboratory
Mail Stop 125-177
4800 Oakgrove Drive
Pasadena, California 91109
(818) 354-5076

Professor Calvin T. Swift
Professor
University of Massachusetts
at Amherst
Microwave Remote Sensing Laboratory
College of Engineering
Amherst, MA 01003
(413) 545-2136
OMNET - C.SWIFT

Professor Edward Thornton
Superintendent
Naval Postgraduate School
Department of Oceanography
(68)
Monterey, CA 93943
(408) 646-2847

Mr. H. Minh Tran
Ocean Research and Engineering
255 South Marengo Avenue
Pasadena, California 91101
(818) 568-1800
OMNET - O.SHEMDIN

Mr. Jim West
University of Kansas
Center for Research, Inc.
Campus West
2291 Irving Hill Drive
Lawrence, Kansas 66045-2969
(913) 864-4835

Dr. Jon Wright
Staff Scientist
La Jolla Institute
10280 North Torrey Pines Road
La Jolla CA 92038
(619) 587-6019
OMNET - J.WRIGHT

Dr. Howard Zebker
Jet Propulsion Laboratory
4800 Oak Grove
Pasadena California 91109
(818) 354-8780